Gaia DR2 astrometry

L. Lindegren[1] J. Hernández[2] A. Bombrun[2] S. Klioner[3]
U. Bastian[4] M. Ramos-Lerate[2] A. de Torres[2] H. Steidelmüller[3]
C. Stephenson[2] D. Hobbs[1] U. Lammers[2] M. Biermann[4]

[1]Lund Observatory, Lund
[2]European Space Agency/ESAC, Madrid
[3]Lohrmann Observatorium, Dresden
[4]Astronomisches Rechen-Institut, Heidelberg

IAU 30 GA – Division A: Fundamental Astronomy
Vienna, 2018 August 27

lennart@astro.lu.se

Main references

A18 F. Arenou et al. (2018):
Gaia DR2: Catalogue validation (link)

L18 L. Lindegren et al. (2018):
Gaia DR2: The astrometric solution (link)

\+ New material

This is an extended version of the presentation at IAU 30 GA. Extra material is marked with a red footer. The original (short) version is on the IAU Division A pages
www.iau.org/science/scientific_bodies/divisions/A/

Outline

Formal uncertainty in parallax

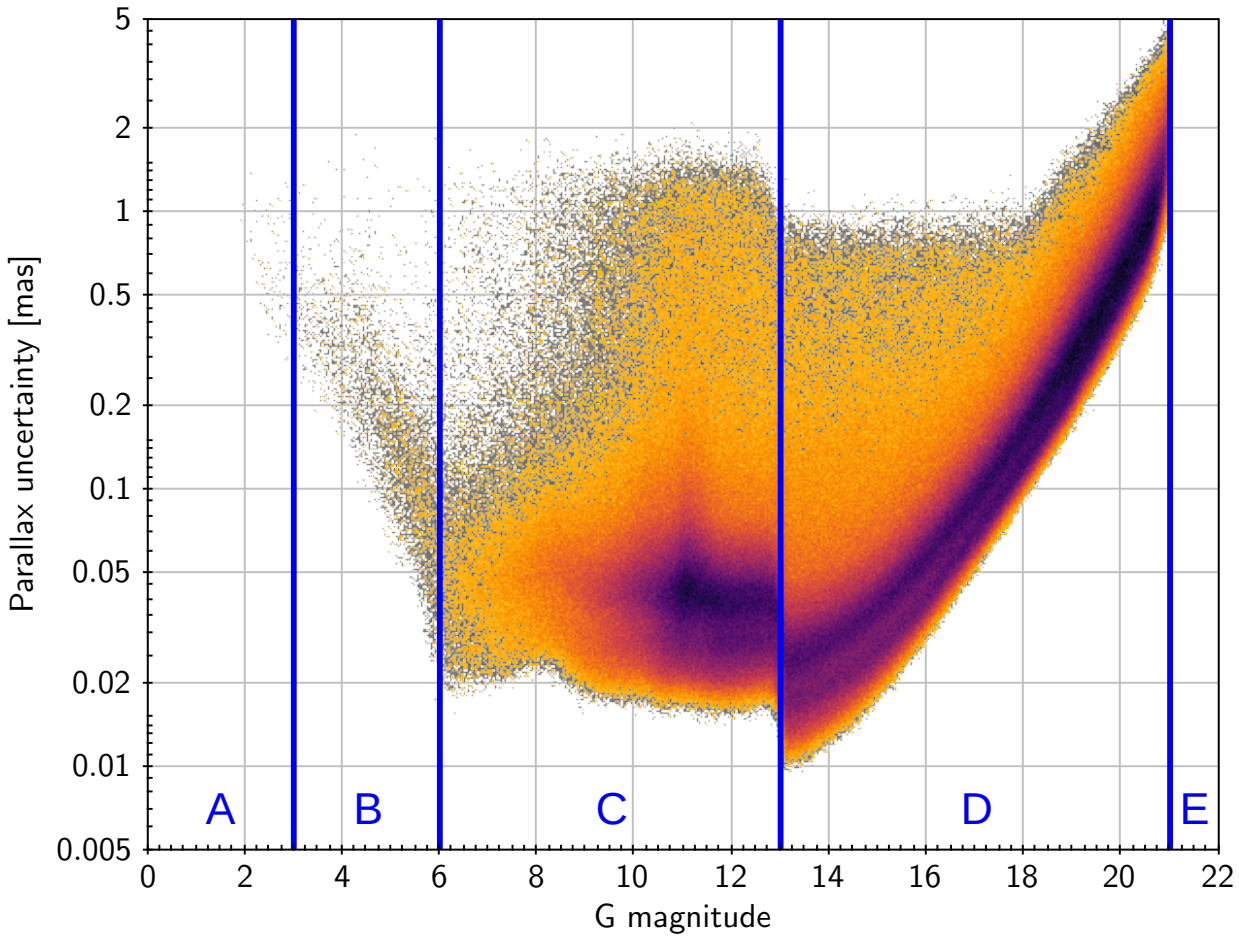

Regimes of G:

- A: Too bright
- B: Partly saturated (unreliable)
- C: Detector and calibration limited
- D: Photon limited
- E: Too faint (not published)

Formal uncertainties in *Gaia* DR2 were estimated from the internal consistency of measurements and do not represent the total error

Random and systematic errors

A useful model for the total (external) error in parallax for source i is

$$\varpi_i^{\mathrm{DR2}} - \varpi_i^{\mathrm{true}} = r_i + s(\alpha, \delta, G, C, \dots) \quad (1)$$

Random error r_i:

- On average zero, uncorrelated between different sources
- Formal uncertainty σ_i is a (possibly underestimated) estimate of its standard deviation: $\sigma_r = k\sigma_i$ with correction factor $k \gtrsim 1.0$

Systematic error s:

- May depend on several variables (position, magnitude, colour, ...)
- Same for sources with sufficiently similar position, magnitude, etc
- Mean value is the parallax zero point ϖ_0
- Variance is σ_s^2

Random and systematic errors

In this model the external (total) uncertainty becomes

$$\sigma_{\rm ext} = \sqrt{k^2\sigma_i^2 + \sigma_s^2} \qquad (2)$$

- Astrophysical applications using likelihood or Bayesian methods require the probability density of the total error $e_i = \varpi_i^{\rm DR2} - \varpi_i^{\rm true}$
- Most conservative assumption:
  e_i is Gaussian with mean value ϖ_0 and standard deviation $\sigma_{\rm ext}$

External data must be used to "calibrate" the model
by estimating ϖ_0, k and σ_s (see next slides)

Values may depend on the sample used

An aside about TGAS

In the Tycho-Gaia Astrometric Solution (TGAS) of *Gaia* DR1, the published uncertainties represent the total (external) errors, and were calculated by applying an expression like (2) to the internal uncertainties. For TGAS the parameters $k = 1.4$ and $\sigma_s = 0.2$ mas were obtained from a comparison with HIPPARCOS parallaxes as described in Appendix B of Lindegren et al. A&A 595, A4 (2016).

For Gaia DR2 no such external calibration was applied before the release.

There is consequently an important difference between DR1 and DR2 when it comes to the interpretation of the astrometric uncertainties as given in the *Gaia* Archive:

- For *Gaia* DR1 (TGAS) the published uncertainties correspond to σ_{ext}
- For *Gaia* DR2 the published uncertainties correspond to σ_i

Parallax zero point (ϖ_0)

The zero point ϖ_0 is the expected measured parallax for a source at infinity; it should thus be *subtracted* from the catalogue value.

As a global average, $\varpi_0 \equiv \langle s \rangle \simeq -0.03$ mas, but:

- s definitely depends on (α, δ)
- s probably depends of G
- s may depend of $C = G_{\mathrm{BP}} - G_{\mathrm{RP}}$
- the dependence is probably multivariate, $s(\alpha, \delta, G, C, \ldots)$

No general recipe can be given
for the correction of the zero point

Systematics $s(\alpha, \delta)$ on large scales

QSO parallaxes smoothed by a Gaussian beam ($\sigma = 3.7°$)
(only $|\sin b| > 0.2$ shown)

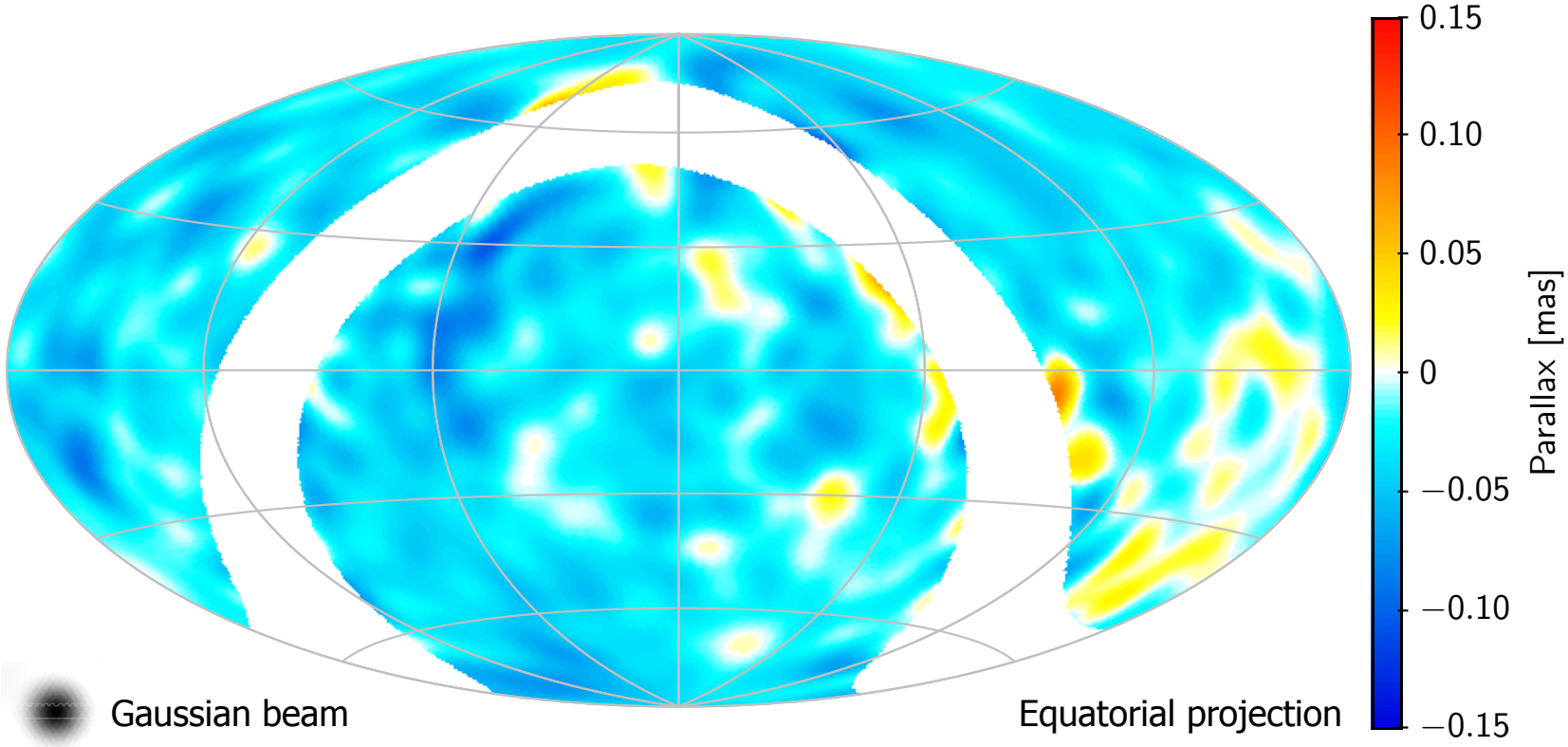

Mean value = −0.030 mas, RMS of smoothed values = 0.020 mas

Systematics $s(\alpha, \delta)$ on small scales

Quasi-periodic patterns imprinted by the *Gaia* scanning law

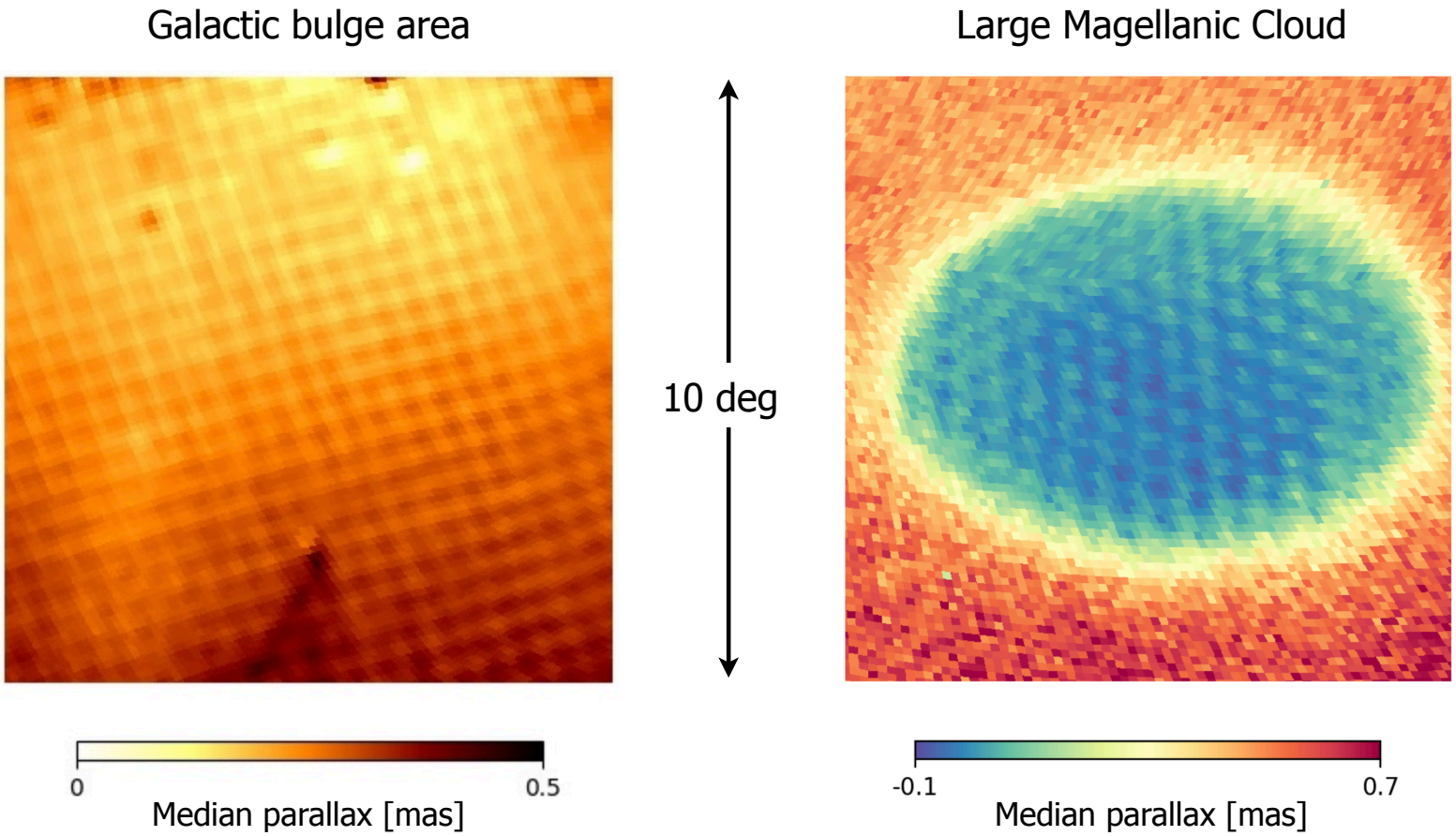

Characteristic period $\simeq$ 0.6 deg, RMS variation $\simeq$ 0.02–0.04 mas

(A18, Figs. 12–13)

Spatial covariance function $V_\varpi(\theta)$

$\theta = 0$ to 180°

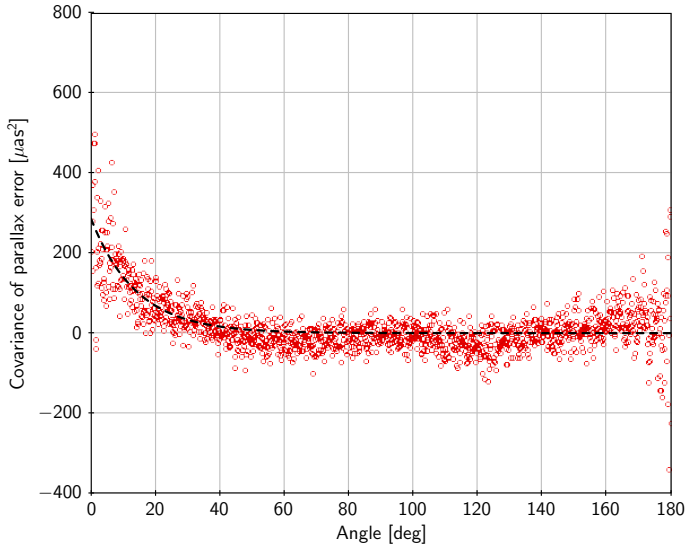

$\theta = 0$ to 7°

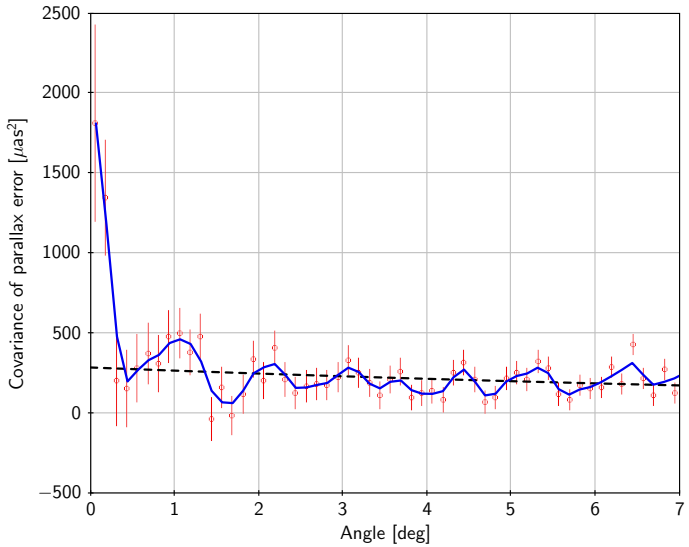

(L18, Fig. 14)

- $V_\varpi(\theta)$ is a statistical description of the systematic error $s(\alpha, \delta, \dots)$ on different scales, equivalent to an angular power spectrum
- The total variance is $V_\varpi(0) = \sigma_s^2$, from which $\sigma_s = 0.043$ mas
- $V_\varpi(\theta)$ and $V_\mu(\theta)$ make it possible to estimate the systematic uncertainty of the mean parallax or proper motion of a cluster (slides 18–27)

Parallax systematics vs. magnitude

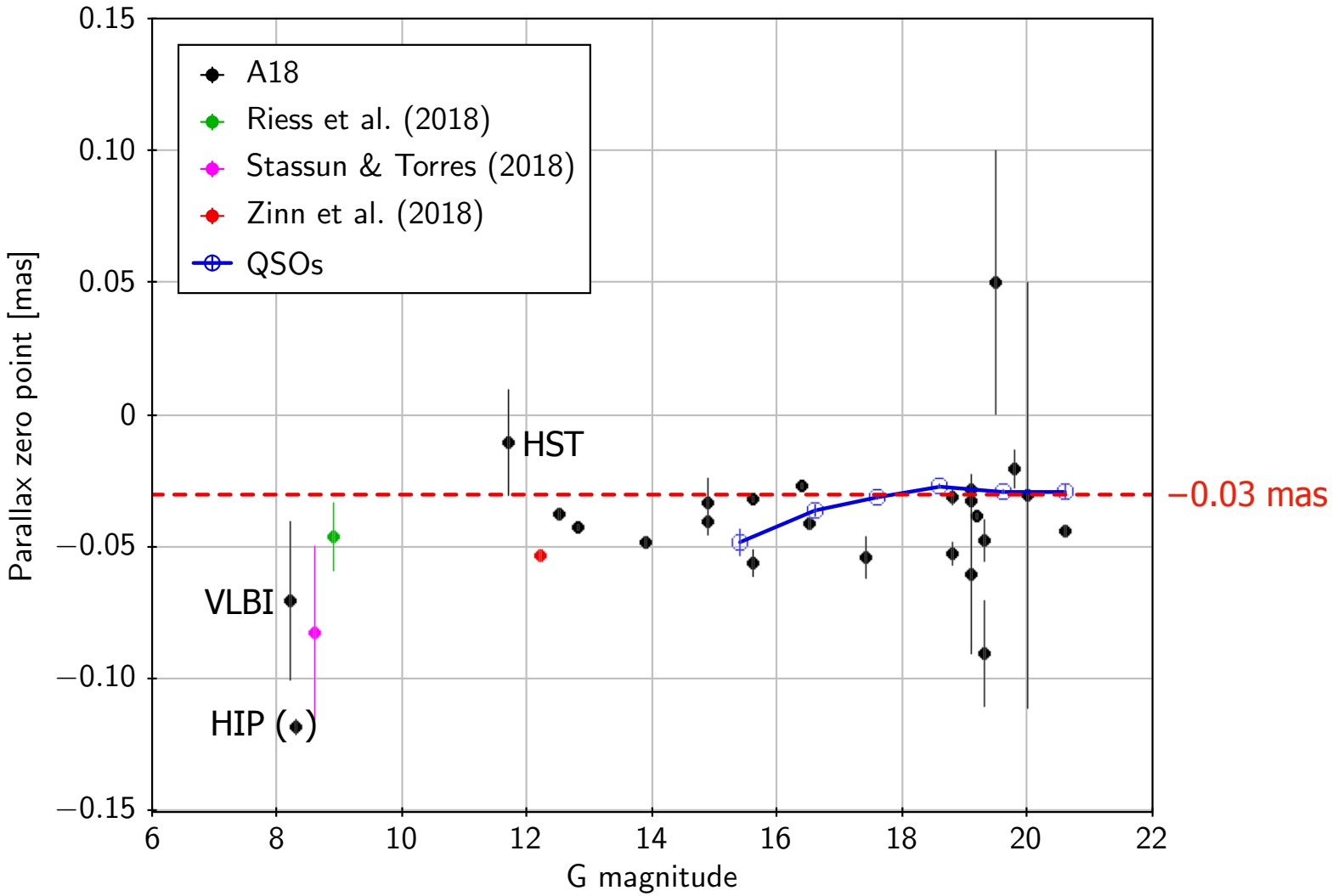

A more negative zero point may apply to sources brighter than the QSOs

Parallax systematics vs. colour

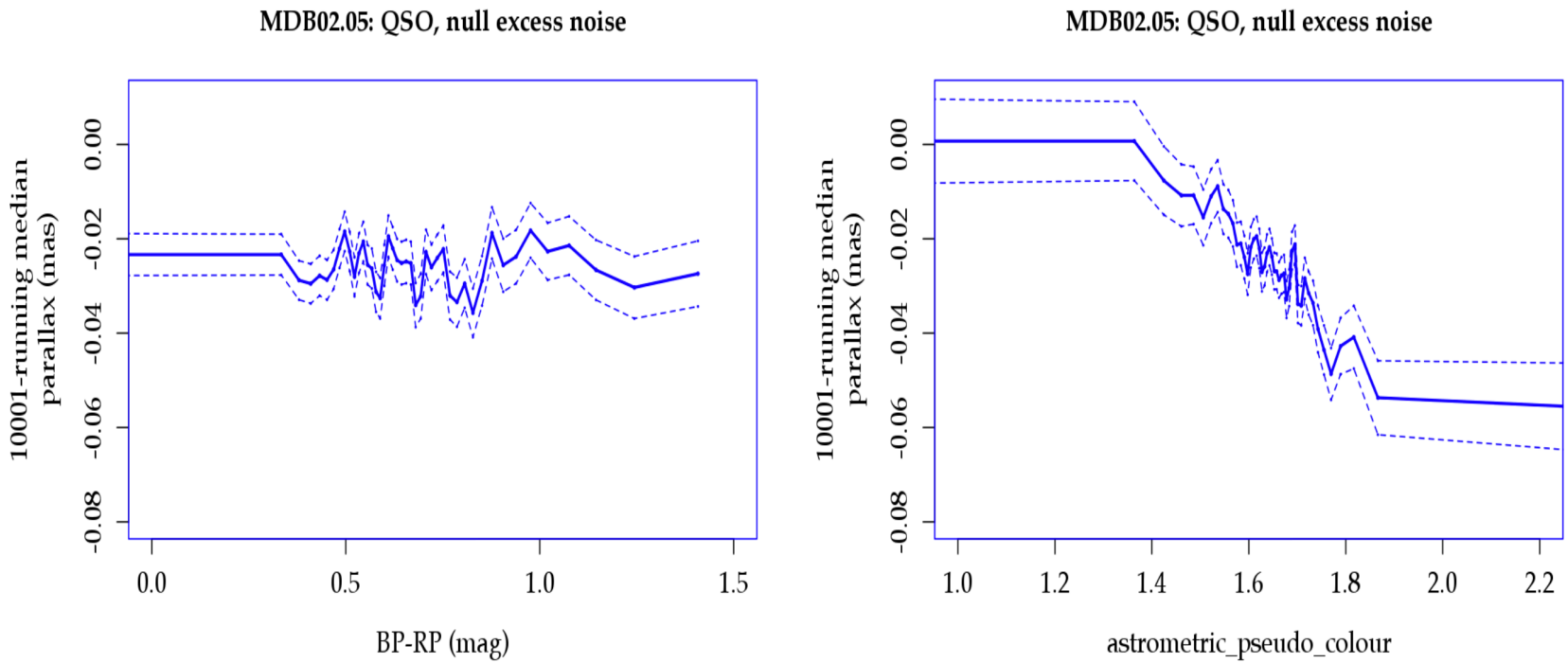

(A18, Fig. 18, top)

Quasar data give no clear indication of a systematic dependence on $G_{BP} - G_{RP}$ for these faint sources (left panel). The strong dependence on the astrometric pseudo-colour right panel) is probably caused by the joint determination of these two parameters in the astrometric solutions (see Sect. 3.1 in L18) and cannot be interpreted as a colour effect.

Estimating k and σ_s in the error model

From Eq. (2) the ratio of external to internal (formal) errors is

$$\frac{\sigma_{\rm ext}}{\sigma_i} = \sqrt{k^2 + \left(\frac{\sigma_s}{\sigma_i}\right)^2} \tag{3}$$

A18 and others have estimated this ratio for various samples covering different magnitude ranges.

- Estimating k:
  in the faint limit photon noise dominates ($\sigma_i \gg \sigma_s$) so $\sigma_{\rm ext}/\sigma_i \to k$
- Estimating σ_s (two methods):
  – from $\sigma_{\rm ext}/\sigma_i$ of brighter sources when k is known, using Eq. (3)
  – from the spatial covariance $V_\varpi(\theta)$, using that $V_\varpi(0) = \sigma_s^2$

Estimating k and σ_s

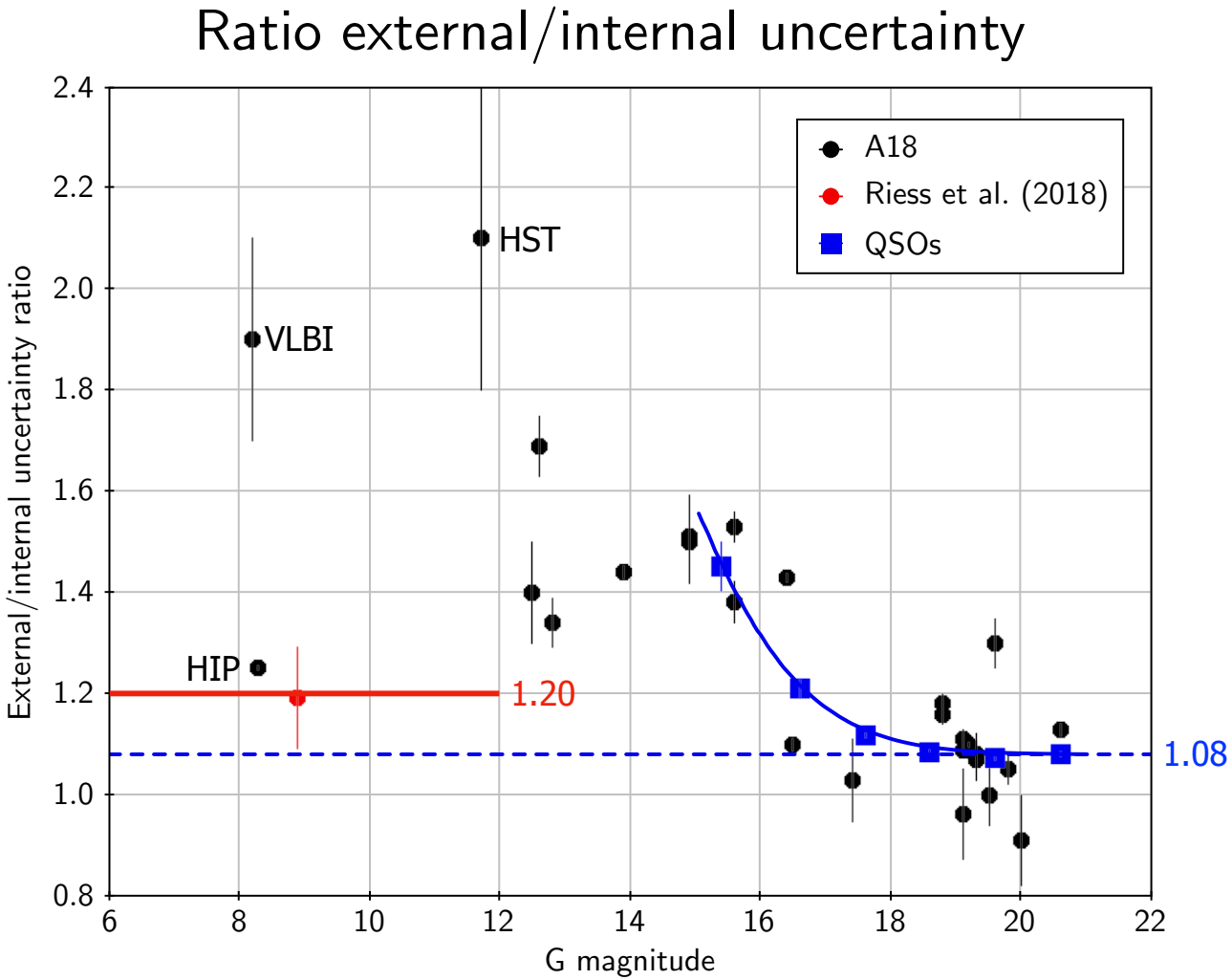

k and σ_s estimated from $\sigma_{\text{ext}}/\sigma_i$ vs. G:

Quasars (blue):

$k = 1.08$

$\sigma_s = 0.043$ mas

Bright stars (red):

$k = 1.08$ (assumed)

$\sigma_s = 0.021$ mas

A tentative external "calibration"

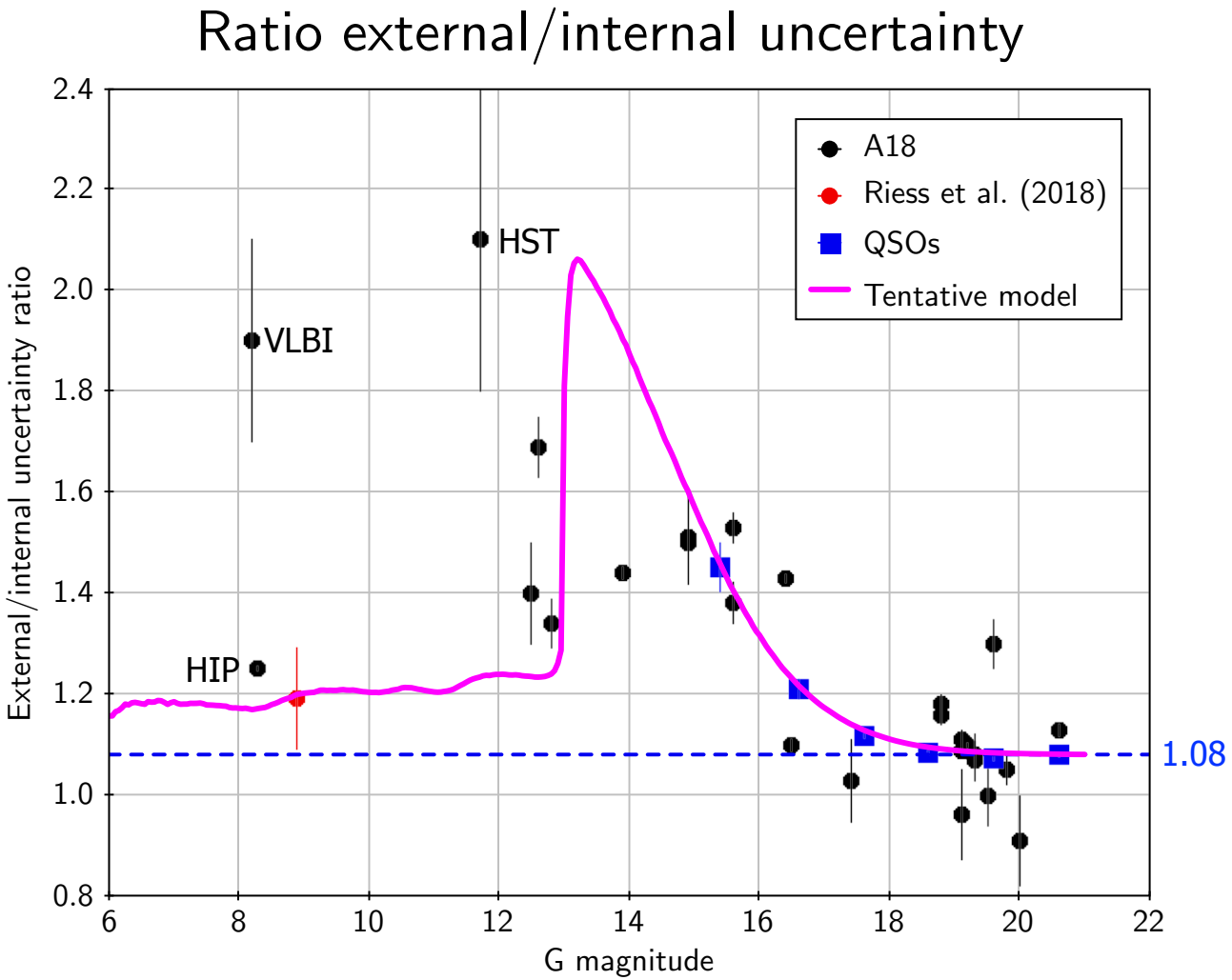

$$\sigma_{\text{ext}} = \sqrt{k^2\sigma_i^2 + \sigma_s^2}$$

Faint ($G \gtrsim 13$):

$k = 1.08$

$\sigma_s = 0.043$ mas

Bright ($G \lesssim 13$):

$k = 1.08$

$\sigma_s = 0.021$ mas

The model may be too pessimistic for $G \simeq 13$ to 15

A tentative external "calibration"

σ_i

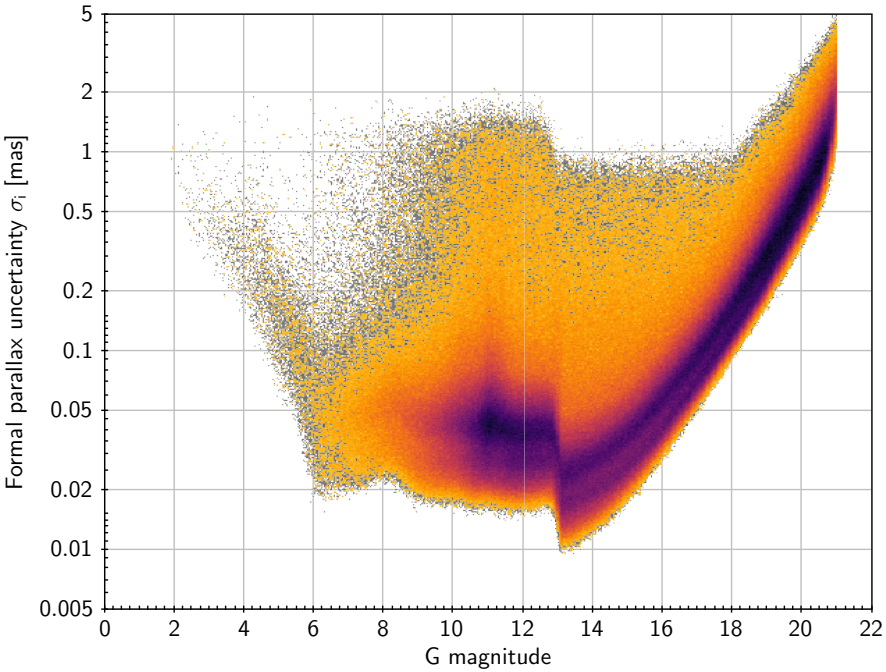

$\sigma_{\text{ext}} = \sqrt{k^2\sigma_i^2 + \sigma_s^2}$

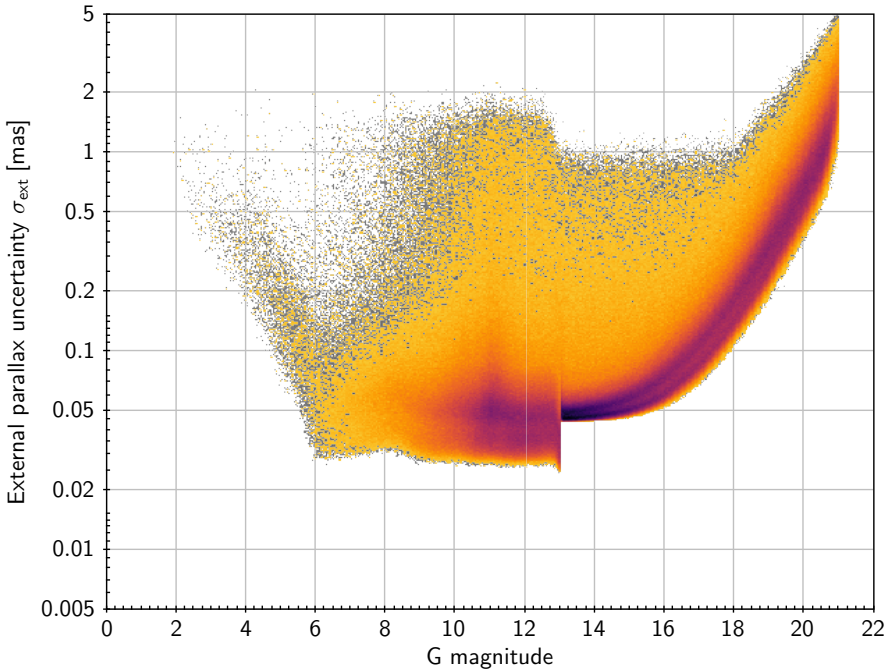

$k = 1.08$ and $\sigma_s = 0.021$ mas ($G < 13$) or 0.043 mas ($G > 13$)

The model may be too pessimistic for $G \simeq 13$ to 15

Spatial covariance of parallax errors

For sources $i \neq j$ separated by angle θ the covariance of QSO parallaxes is

$$V_\varpi(\theta) = \mathrm{E}\left[(\varpi_i - \varpi_0)(\varpi_j - \varpi_0)\right] \tag{4}$$

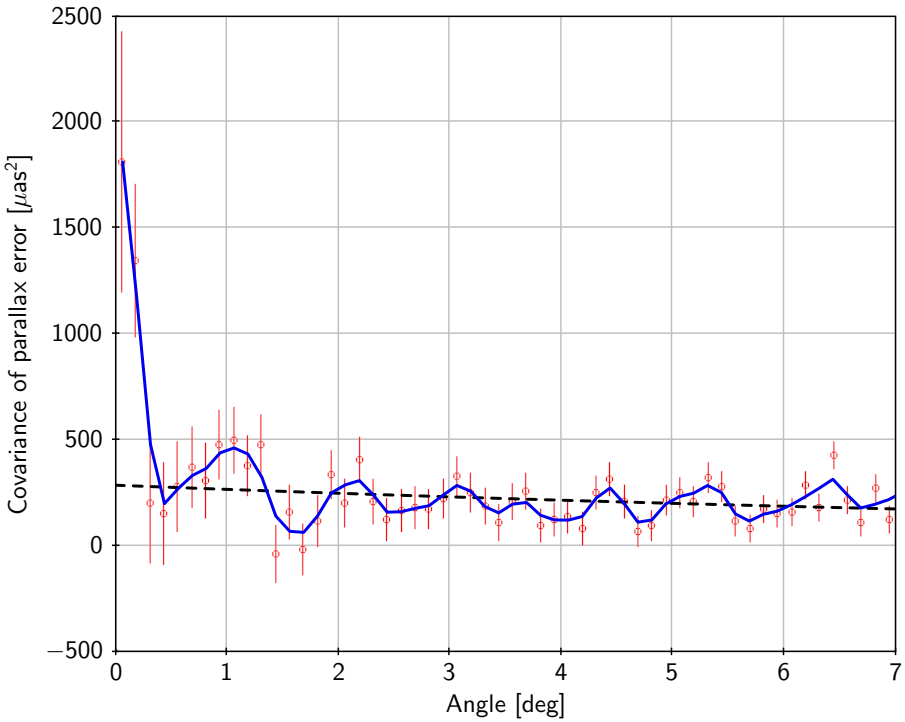

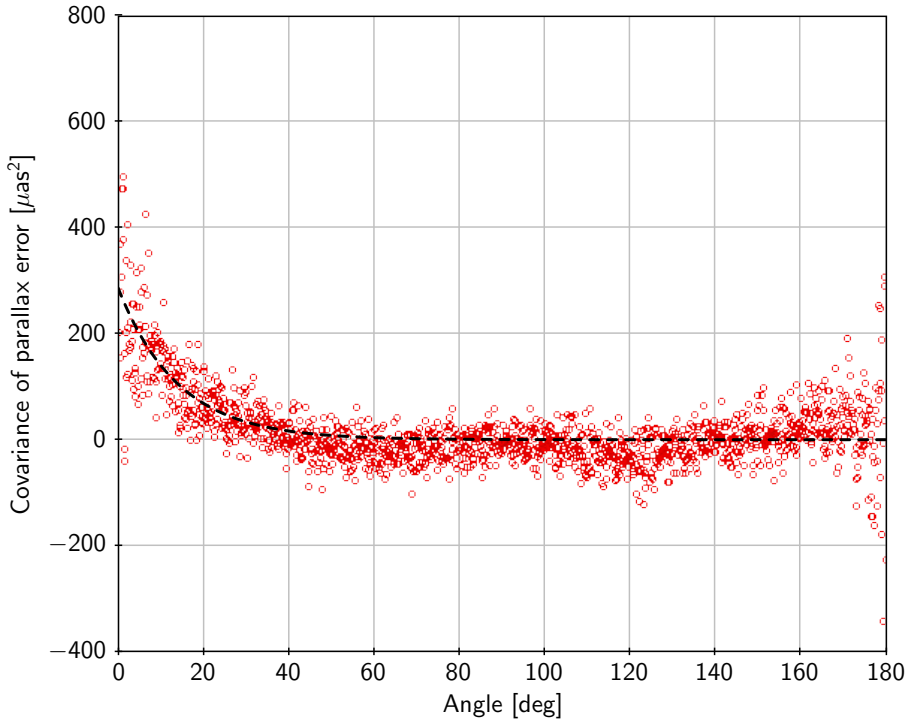

The function $V_\varpi(\theta)$ estimated from quasar parallaxes (L18, Fig. 14)

Correlated errors: Using $V_\varpi(\theta)$

For two sources i, j the random errors are assumed to be uncorrelated, while the systematic errors are not. The position-dependent part of s is modelled by the spatial covariance function $V_\varpi(\theta)$; thus

$$\mathrm{E}\left[(\varpi_i - \varpi_0)(\varpi_j - \varpi_0)\right] = \begin{cases} k^2\sigma_i^2 + V_\varpi(0) & \text{if } i = j \\ V_\varpi(\theta_{ij}) & \text{if } i \neq j \end{cases} \tag{5}$$

where θ_{ij} is the angle between the sources. Note: $V_\varpi(0) = \sigma_s^2$.

The spatial covariance functions provide an approximate *joint* error model for a sample of sources, which makes it possible to treat correlated errors e.g. in a cluster.

Tables of $V_\varpi(\theta)$ and $V_\mu(\theta)$, corresponding to Figs. 14 and 15 in L18, are available on the ESA *Gaia* Known issues page.

Notes on Eq. (5)

The error model formulated for parallaxes can be used for the proper motions as well, with the global rotation replacing the parallax zero point.

Equation (5) makes some strong assumptions on V_ϖ, in particular:
(i) that it is essentially independent of G (in contrast to σ_i), and
(ii) that it is spatially and rotationally invariant, i.e. only depends on θ.

Assumption (i) is reasonable if the systematics mainly come from calibration and attitude errors, which could be independent of G at least in some range. There is empirical support for this: the $V_\mu(\theta)$ derived from the proper motion errors of bright sources (slide 33) turns out to be very similar to the one derived from the proper motions of faint quasars.

Assumption (ii) is more based on necessity than theoretical expectation, given the inhomogeneity of the *Gaia* scanning. It could nevertheless provide a useful approximation, as illustrated in the examples below.

Error propagation including systematics

Let $h(\varpi_1, \varpi_2, \ldots, \varpi_n)$ be some arbitrary function of the measured parallaxes for a sample of n sources. Using the error model in Eq. (5) and linear propagation of the errors (with $c_i = \partial h / \partial \varpi_i$), the variance of h is obtained as

$$\sigma_h^2 = \sum_{i=1}^{n} c_i^2 (k^2 \sigma_i^2 + V_\varpi(0)) + 2 \sum_{i=2}^{n} \sum_{j=1}^{i-1} c_i c_j V_\varpi(\theta_{ij}) \qquad (6)$$

The first term is the "random" contribution from the individual uncertainties $\sigma_{\rm ext}$; the second is the "systematic" contribution from the spatially correlated errors. Note: $V_\varpi(0) = \sigma_s^2$.

[The second term can in principle be negative; however, in most cases where spatial correlations are a concern it is positive, and for large n often the dominant term.]

Example 1: Mean parallax of a cluster

The (unweighted) mean parallax for a cluster of n stars is $s(\varpi_1, \varpi_2, \ldots, \varpi_n) = n^{-1} \sum_{i=1}^{n} \varpi_i$; thus $c_i = n^{-1}$ and

$$\sigma_h^2 = \frac{1}{n}\left(k^2\langle\sigma_i^2\rangle + V_\varpi(0)\right) + \frac{n-1}{n}\langle\langle V_\varpi(\theta_{ij})\rangle\rangle \qquad (7)$$

where $\langle\rangle$ denotes an average over the n sources and $\langle\langle\rangle\rangle$ an average over the $n(n-1)/2$ non-redundant pairs. Note: $V_\varpi(0) = \sigma_s^2$.

Notes:

- While the first term depends strongly on both n and G (via σ_i), the second term essentially depends only on the spatial distribution of the sources. For large enough n the second term will dominate.
- A corresponding formula holds for the mean proper motion in α or δ, with V_μ replacing V_ϖ.

Example 2: Proper motion gradient

In local plane coordinates (x, y) the p.m. gradients $b = \partial\mu/\partial x$ etc. (where μ is either $\mu_{\alpha*}$ or μ_δ) may be obtained by least-squares estimation of a and b in $\mu_i \simeq a + bx_i$. If the origin is chosen such that $\sum_{i=1}^{n} x_i = 0$, the (unweighted) LS estimate is $b = \sum_{i=1}^{n} x_i\mu_i / \sum_{i=1}^{n} x_i^2$; thus $c_i = n^{-1}x_i/\langle x^2\rangle$.

With σ_i denoting the uncertainty of μ_i, the variance of the gradient is

$$\sigma_b^2 = \frac{1}{n}\frac{\langle x_i^2(k^2\sigma_i^2 + V_\mu(0))\rangle}{\langle x_i^2\rangle^2} + \frac{n-1}{n}\frac{\langle\langle x_i x_j V_\varpi(\theta_{ij})\rangle\rangle}{\langle x_i^2\rangle^2} \tag{8}$$

Note:

- While the first term depends strongly on both n and G (via σ_i), the second term essentially depends only on the spatial distribution of the sources. For large enough n the second term will dominate.

Numerical examples

The second ("systematic") term in Eq. (7) or (8) was computed for simulated clusters of different angular size R. The number of sources per cluster was always $n = 200$, but the results are almost independent of n.

Two different shapes were considered:

- Uniform disk: sources uniformly distributed in a circle of radius R
- Gaussian disk: sources normally distributed with standard deviation R in each coordinate

Results are shown on slides 25–27.

Simulations made use of tables of $V_\varpi(\theta)$ and $V_\mu(\theta)$, corresponding to Figs. 14 and 15 in L18, available on the ESA *Gaia* Known issues page.

For real clusters one should of course use the actual coordinates (x_i, y_i) and include weights in c_i as required by the specific application.

Average parallax of a cluster

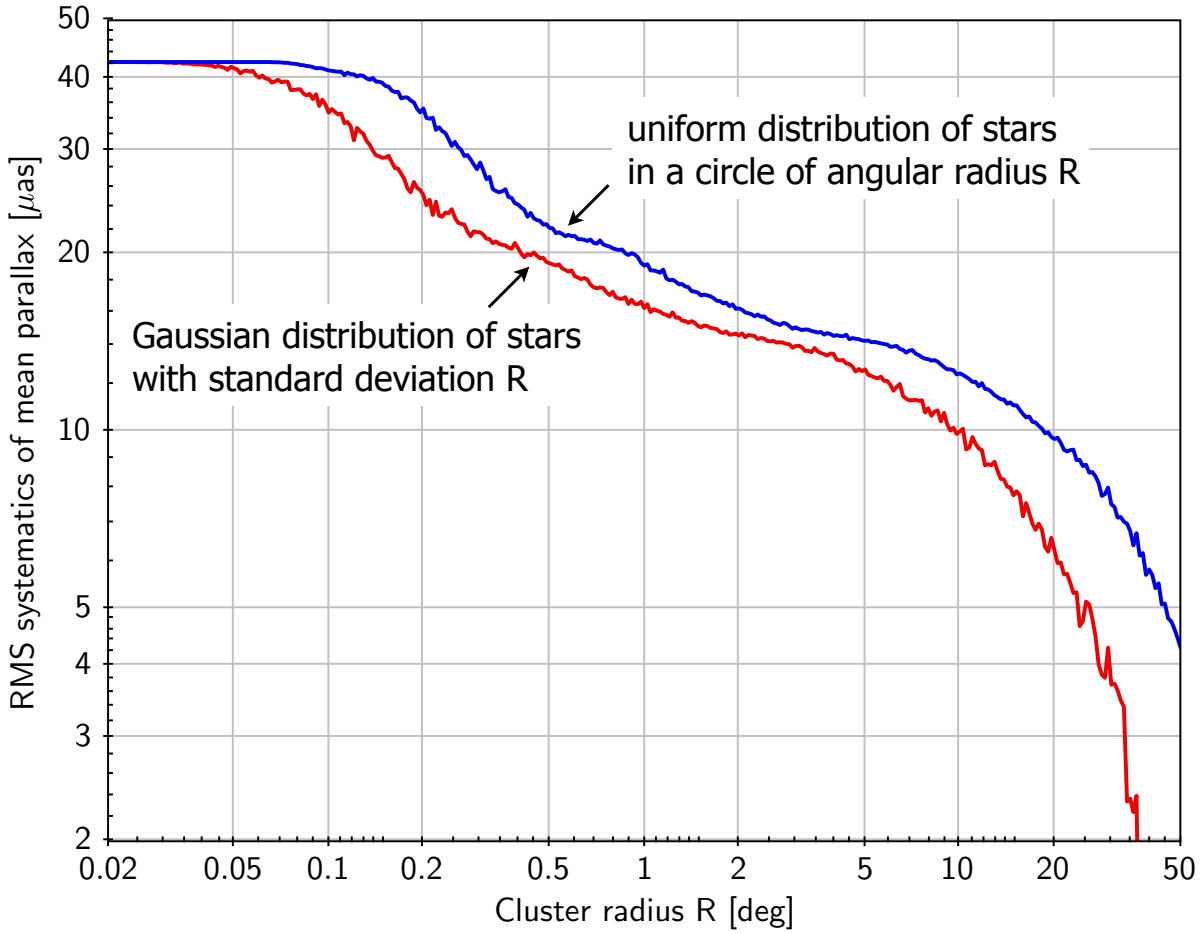

RMS systematics in $\langle \varpi \rangle$ for simulated clusters of different sizes, estimated from the spatial covariance function $V_\varpi(\theta)$

Average proper motion of a cluster

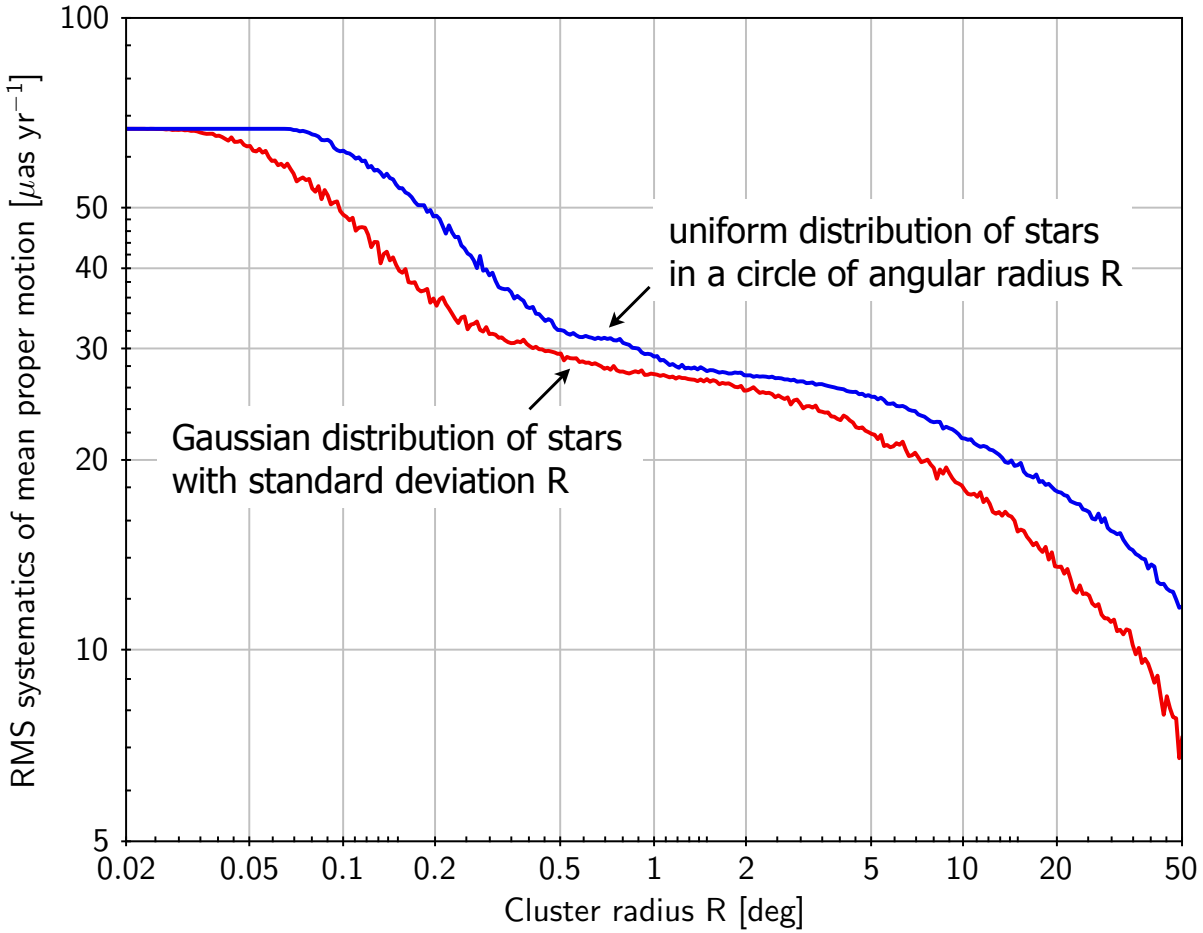

RMS systematics in $\langle \mu_{\alpha *} \rangle$ for simulated clusters of different sizes, estimated from the spatial covariance function $V_\mu(\theta)$

Proper motion gradient in a cluster

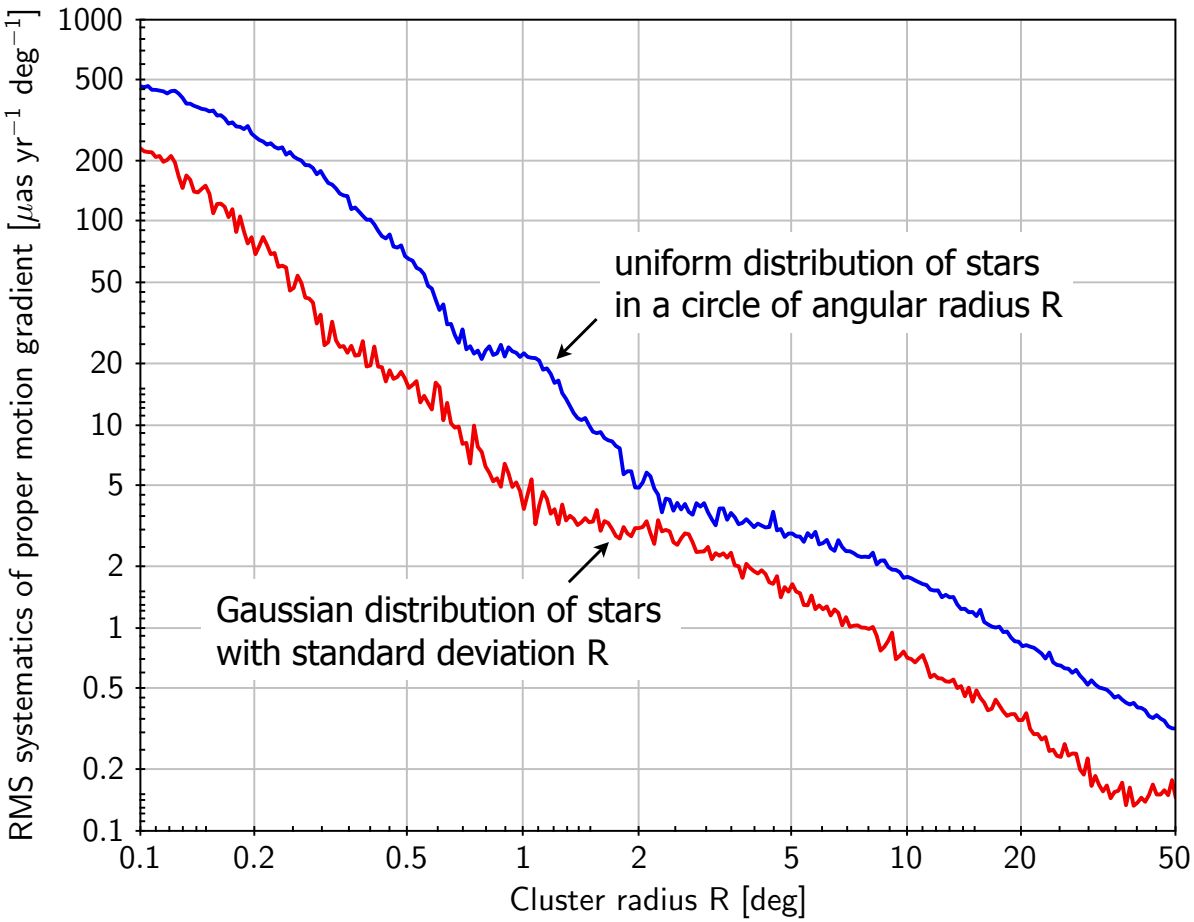

RMS systematics in $\partial\mu_{\alpha*}/\partial\alpha*$ for simulated clusters of different sizes, estimated from the spatial covariance function $V_\mu(\theta)$

Systematics in proper motions

Main points:

- Systematics exist on large and small scales similar to the parallax
- For faint sources the reference frame is effectively non-rotating
- For $G \lesssim 12$ the proper motions have a significant ($\sim$0.15 mas yr^{-1}) rotation bias

Systematics in p.m. (faint sources)

Large-scale systematics for QSOs ($G \gtrsim 18$ mag)

R.A.

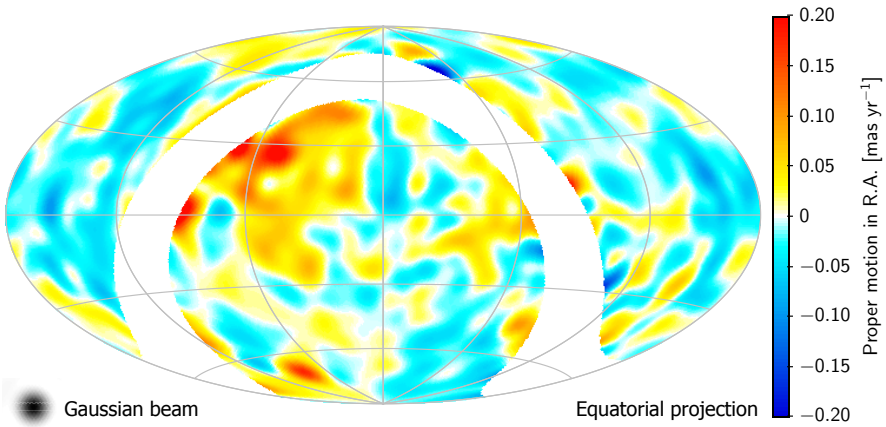

Dec.

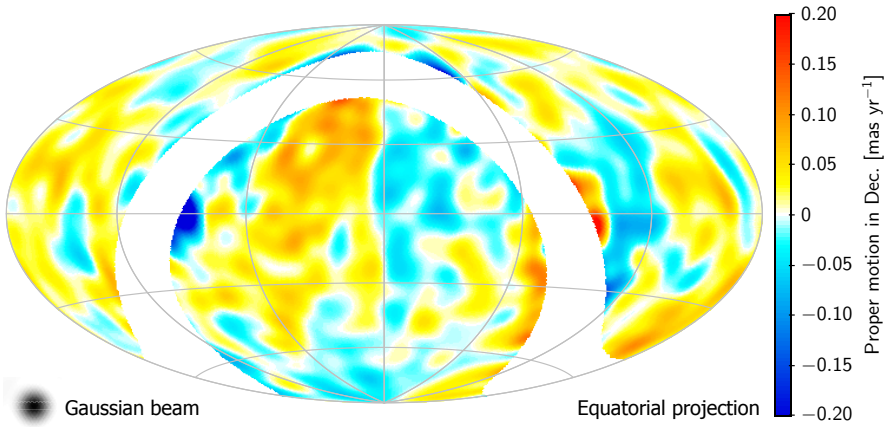

Smoothed values [mas yr^{-1}]:

	R.A.	Dec.
Mean	$\pm$0.000	+0.011
RMS	0.039	0.037

Systematics in p.m. (bright sources)

Large-scale systematics for bright stars ($G \lesssim 12$)

R.A.

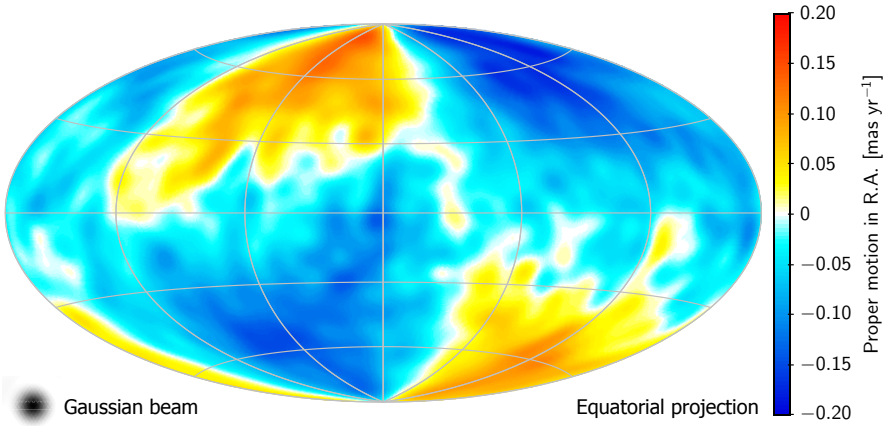

Dec.

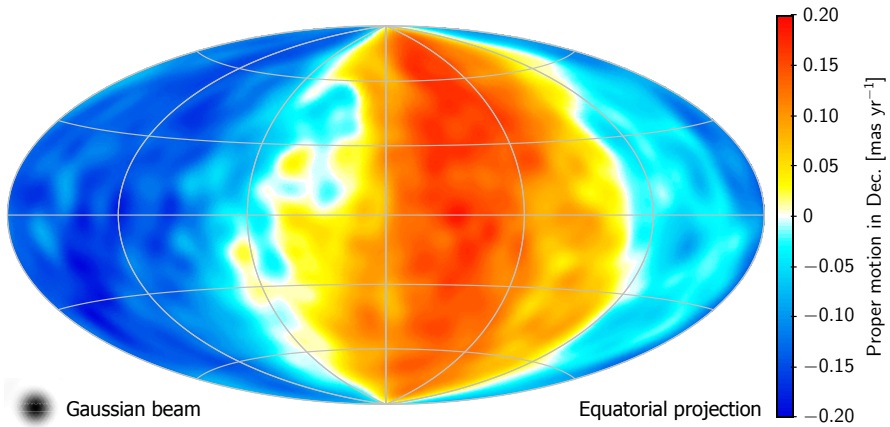

Smoothed $\Delta\mu_{\alpha*}$, $\Delta\mu_\delta$ calculated for the HIPPARCOS subset of *Gaia* DR2

$$\left.\begin{aligned} \Delta\mu_{\alpha*} &= \mu_{\alpha*}^{\mathrm{DR2}} - (\alpha^{\mathrm{DR2}} - \alpha^{\mathrm{HIP}})\cos\delta/(24.25\ \mathrm{yr}) \\ \Delta\mu_\delta &= \mu_\delta^{\mathrm{DR2}} - (\delta^{\mathrm{DR2}} - \delta^{\mathrm{HIP}})/(24.25\ \mathrm{yr}) \end{aligned}\right\} \quad (9)$$

Very clear signature of global rotation $\simeq 0.15$ mas yr^{-1} (cf. L18, Fig. 4)

The maps on slide 30 are based on the positions at epoch J1991.25 for about 115 000 sources in the HIPPARCOS catalogue (van Leeuwen 2007) cross-matched with *Gaia* DR2. At epoch J1991.25 the HIPPARCOS reference frame was aligned with ICRS to ± 0.6 mas per axis. The alignment error of the *Gaia* DR2 frame for the bright sources at epoch J2015.5 should be negligible in comparison. The proper motions calculated from the position differences divided by 24.25 yr therefore have a global rotation uncertainty of ± 0.025 mas yr^{-1}.

The patterns in slide 30 are highly significant and must be caused by systematics in *Gaia* DR2 affecting the proper motions of bright sources. (Note that HIPPARCOS proper motions were not used in this comparison; they have their own systematics, including a rotation, not discussed here.)

Almost all HIPPARCOS sources have $G < 13$ mag and 99.8% have $G < 12$. It is therefore difficult to determine whether the systematics in *Gaia* DR2 are caused by the use of gated observations ($G \lesssim 12$) or two-dimensional windows ($G \lesssim 13$). Figure 4 in L18 shows a gradual change between $G \simeq 11$ and 13, suggesting an effect of the gates.

The inertial spin of the *Gaia* DR2 proper motion system, as estimated from the sample of HIPPARCOS stars, is

$$\begin{bmatrix}\omega_X\\ \omega_Y\\ \omega_Z\end{bmatrix} = \begin{bmatrix}-0.086 \pm 0.025\\ -0.114 \pm 0.025\\ -0.037 \pm 0.025\end{bmatrix} \text{ mas yr}^{-1} \tag{10}$$

The spin can be removed by means of the formulae

$$\left.\begin{aligned}\mu_{\alpha*} &= \mu_{\alpha*}^{\text{DR2}} + \omega_X \sin\delta\cos\alpha + \omega_Y \sin\delta\sin\alpha - \omega_Z\cos\delta\\ \mu_\delta &= \mu_\delta^{\text{DR2}} - \omega_X\sin\alpha + \omega_Y\cos\alpha\end{aligned}\right\} \tag{11}$$

Important: This correction applies *only* to bright sources. At faint magnitudes there is no net rotation, as shown by the quasars (slide 29). As discussed above, the correction probably applies in full for $G \lesssim 11$ and gradually less for $G = 11$ to 13. For $G = 13$ to 16 there are very few comparison data but probably no correction is needed in that interval.

Proper motions: Large scale systematics

Residual systematics in the proper motions of bright ($G \lesssim 12$) sources after removal of the global rotation

R.A.

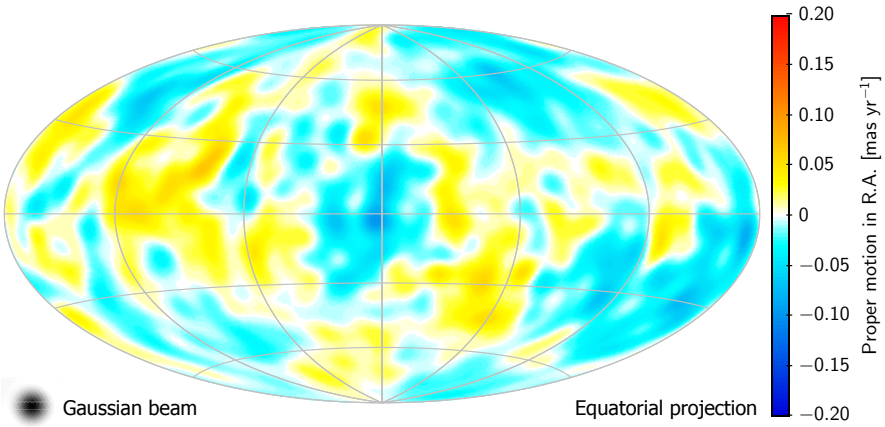

Dec.

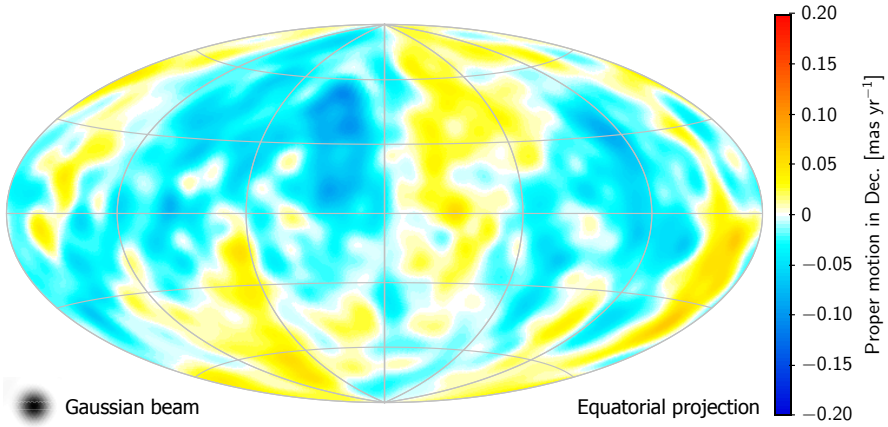

Smoothed values [mas yr^{-1}]:

	R.A.	Dec.
Mean	$\pm$0.000	$-$0.007
RMS	0.024	0.027

Comparing QSOs and bright sources

R.A. Dec.

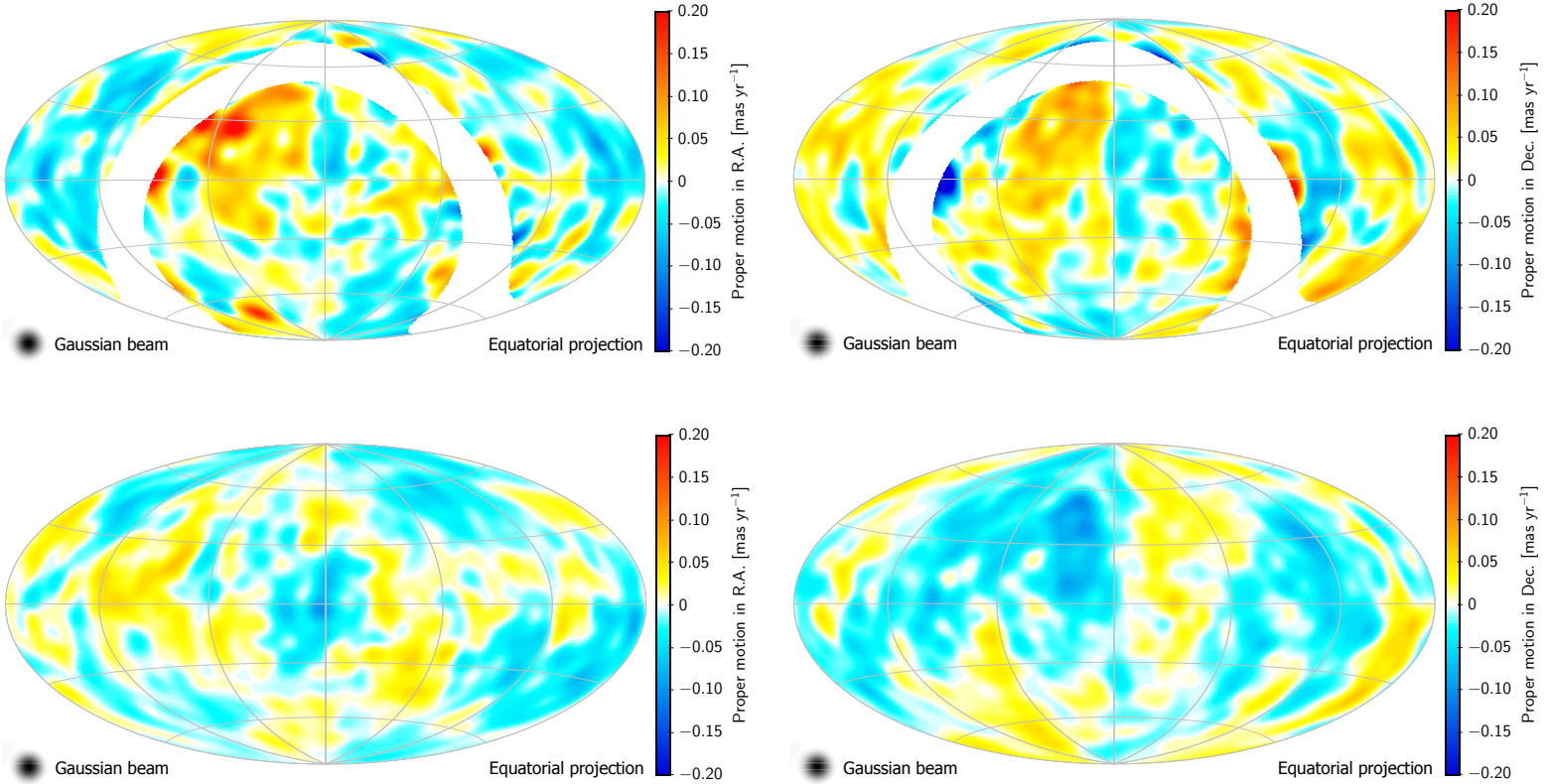

QSOs (slide 29)

Bright sources (slide 33)

There is little or no resemblance in pattern between the faint quasars and bright stars. The scale lengths are similar but the RMS amplitude is a factor 0.7 less for the bright stars.

External uncertainty in position and p.m.

The model on slide 16 agrees well with HIPPARCOS and quasar data at the bright and faint ends, but may be too pessimistic for $G = 13$ to 15.

A higher ratio $\sigma_{\rm ext}/\sigma_i$ applies in crowded areas (A18).

To apply the model also to positions and proper motions, one could assume that σ_s scales as the general uncertainties (e.g. Table B1 in L18):

	$G < 13$	$G > 13$	
Position	$\sigma_s = 0.016$	$\sigma_s = 0.033$	mas
Parallax	$\sigma_s = 0.021$	$\sigma_s = 0.043$	mas
Proper motion	$\sigma_s = 0.032$	$\sigma_s = 0.066$	mas yr^{-1}

$\sigma_s = 0.043$ mas in parallax for $G > 13$ is consistent with the spatial covariance of quasars $V_\varpi(0) \simeq 1850$ μas^2 (L18).

$\sigma_s = 0.066$ mas in proper motion for $G > 13$ is consistent with the spatial covariance of quasars $V_\mu(0) \simeq 4400$ μas^{2}yr^{-2} (L18).

Spatial covariance of proper motion errors

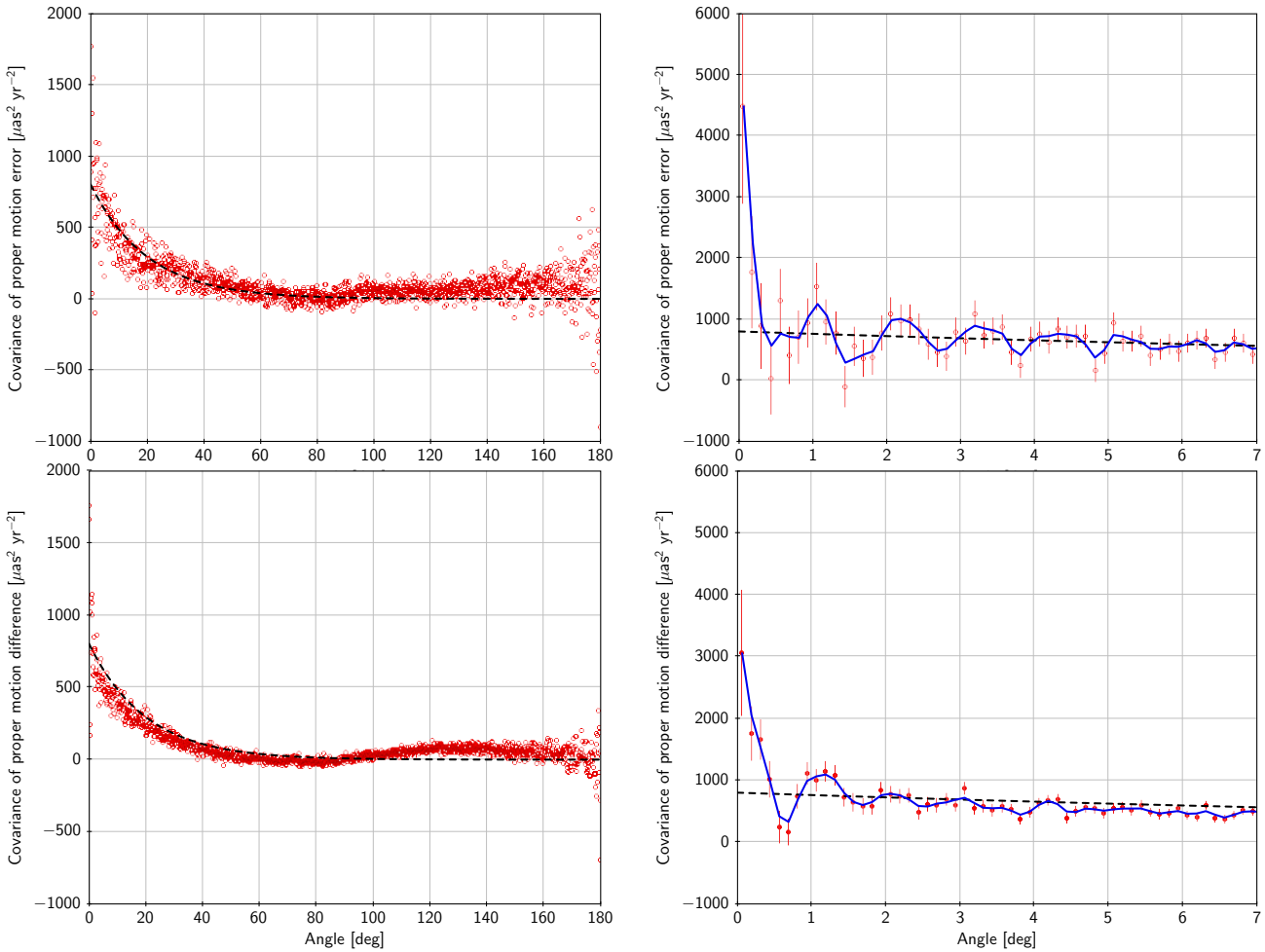

$V_\mu(\theta)$ for QSOs (L18, Fig. 15)

$V_\mu(\theta)$ for bright sources

$V_\mu(\theta)$ calculated from the proper motion differences in Eq. (9) after removing the rotation confirms the similarity in scale lengths, but suggests a higher value $\sigma_s \simeq 55$ μas yr^{-1} for the bright sources.

Quality indicators for the astrometry

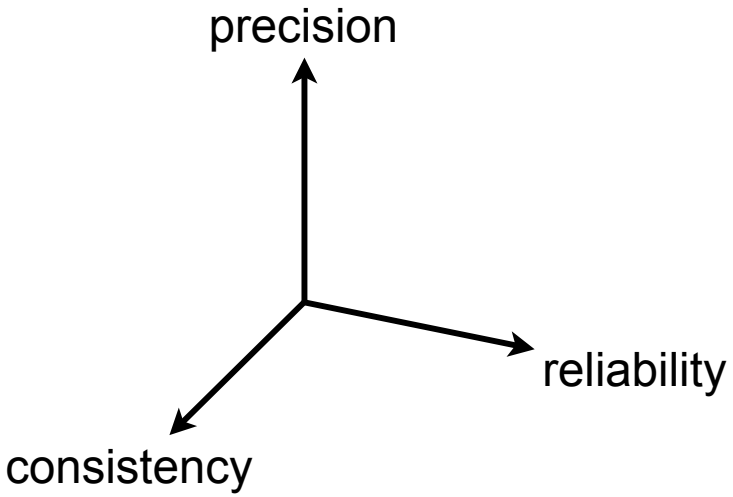

- Precision: `parallax_error`, `pmra_error`, `pmdec_error`, etc. → OK
- Reliability: `visibility_perods_used` (≥ 6 for full solutions) → OK
- Consistency (goodness of fit to the 5-parameter model):
  - ▷ `astrometric_n_bad_obs_al`
  - ▷ `astrometric_gof_al`
  - ▷ `astrometric_chi2_al`
  - ▷ `astrometric_excess_noise`
  - ▷ `astrometric_excess_noise_sig`

  → not recommended

Renormalised Unit Weight Error

- Recommended GoF indicator for *Gaia* DR2 astrometry
- Not given directly in the *Gaia* Archive
- Can be computed from the quantities:

$$\chi^2 = \texttt{astrometric\_chi2\_al}$$
$$N = \texttt{astrometric\_n\_good\_obs\_al}$$
$$G = \texttt{phot\_g\_mean\_mag}$$
$$C = \texttt{bp\_rp} \quad \text{(if available)}$$

- Unit weight error UWE $= \sqrt{\chi^2/(N-5)}$
- Renormalised unit weight error RUWE $=$ UWE$/u_0(G, C)$
- $u_0(G, C)$ is an empirical normalisation factor, provided as a lookup table on the ESA *Gaia* DR2 Known issues page

Normalisation factor $u_0(G, C)$

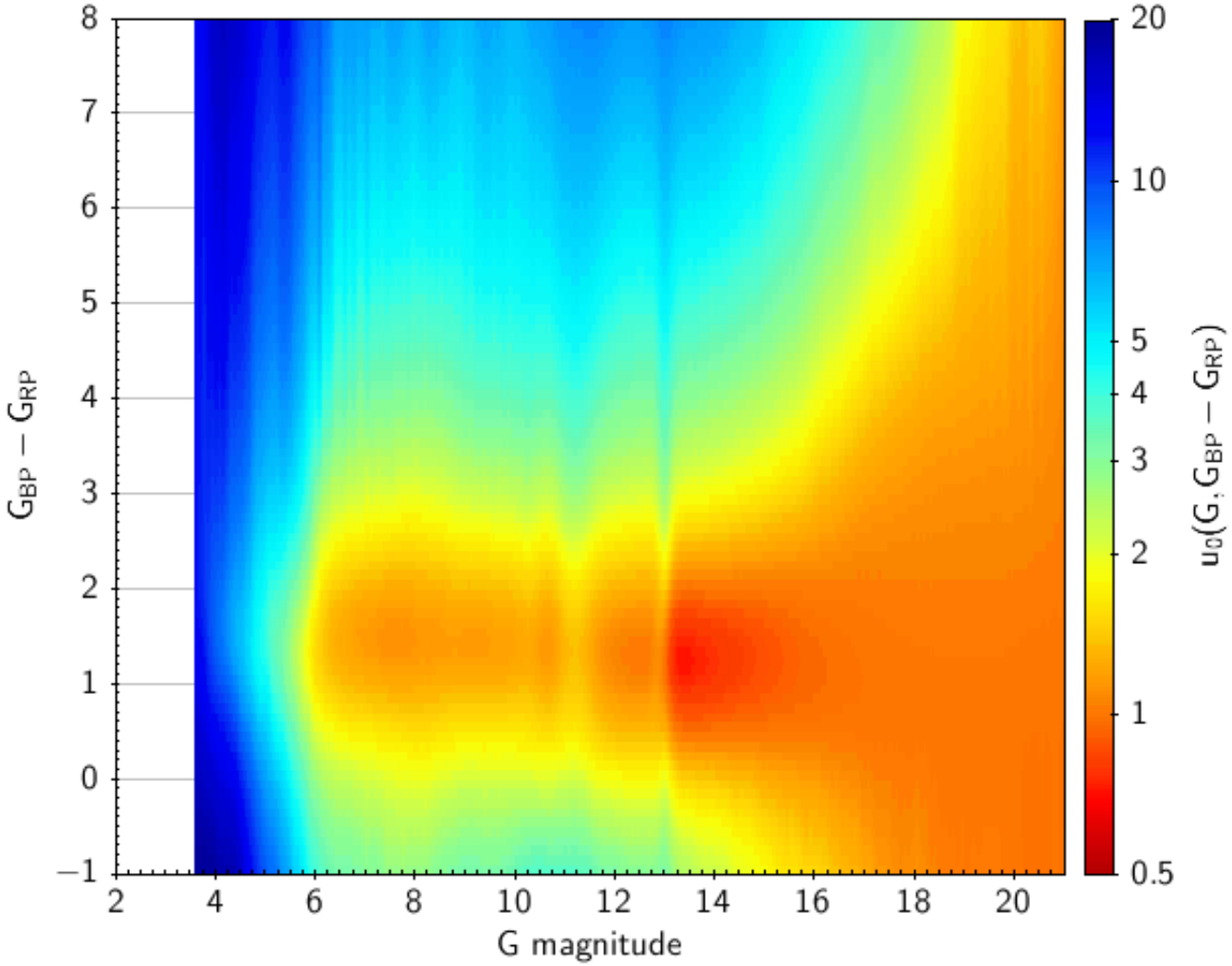

This is essentially the "typical" UWE for a given magnitude and colour

Normalisation factor $u_0(G, C)$

The function $u_0(G, C)$ was determined by sampling *Gaia* DR2 in bins of magnitude and colour, estimating the "typical" UWE (taken as the 41st percentile of the UWE) per bin, and fitting a semi-analytical function.

A separate function $u_0(G)$ should be used for sources without a known colour.

Details are found in the technical note GAIA-C3-TN-LU-LL-124.

Tables of $u_0(G, C)$ and $u_0(G)$ are found on the ESA *Gaia* DR2 Known issues page.

Illustrating the use of RUWE

HRD for sources nominally within 100 pc

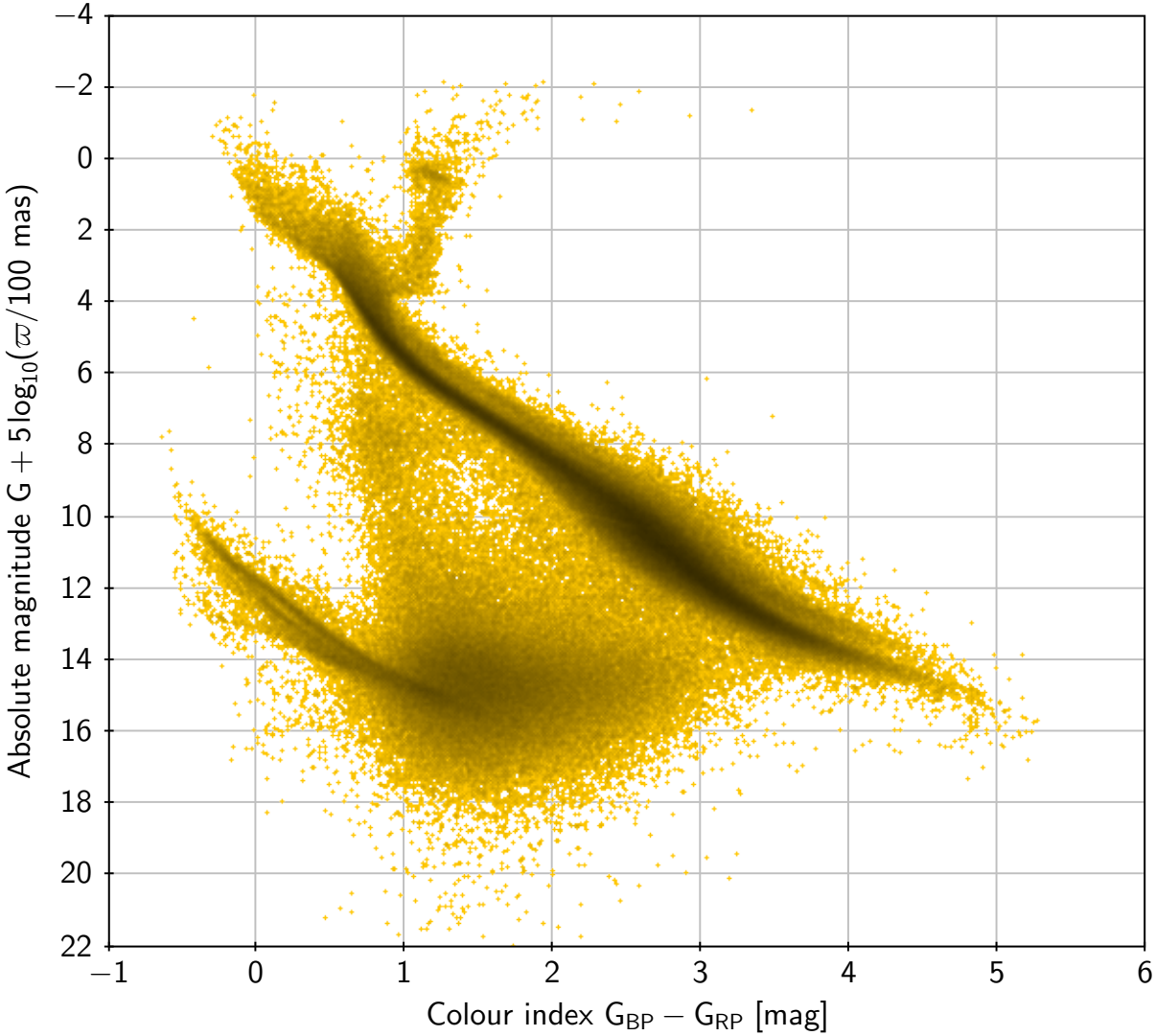

Selection:

$\varpi > 10$ mas
$\varpi/\sigma_\varpi > 10$
SNR > 10
in BP and RP

No filter on GoF

(338 833 sources)

Statistics for the $\varpi > 10$ mas sources

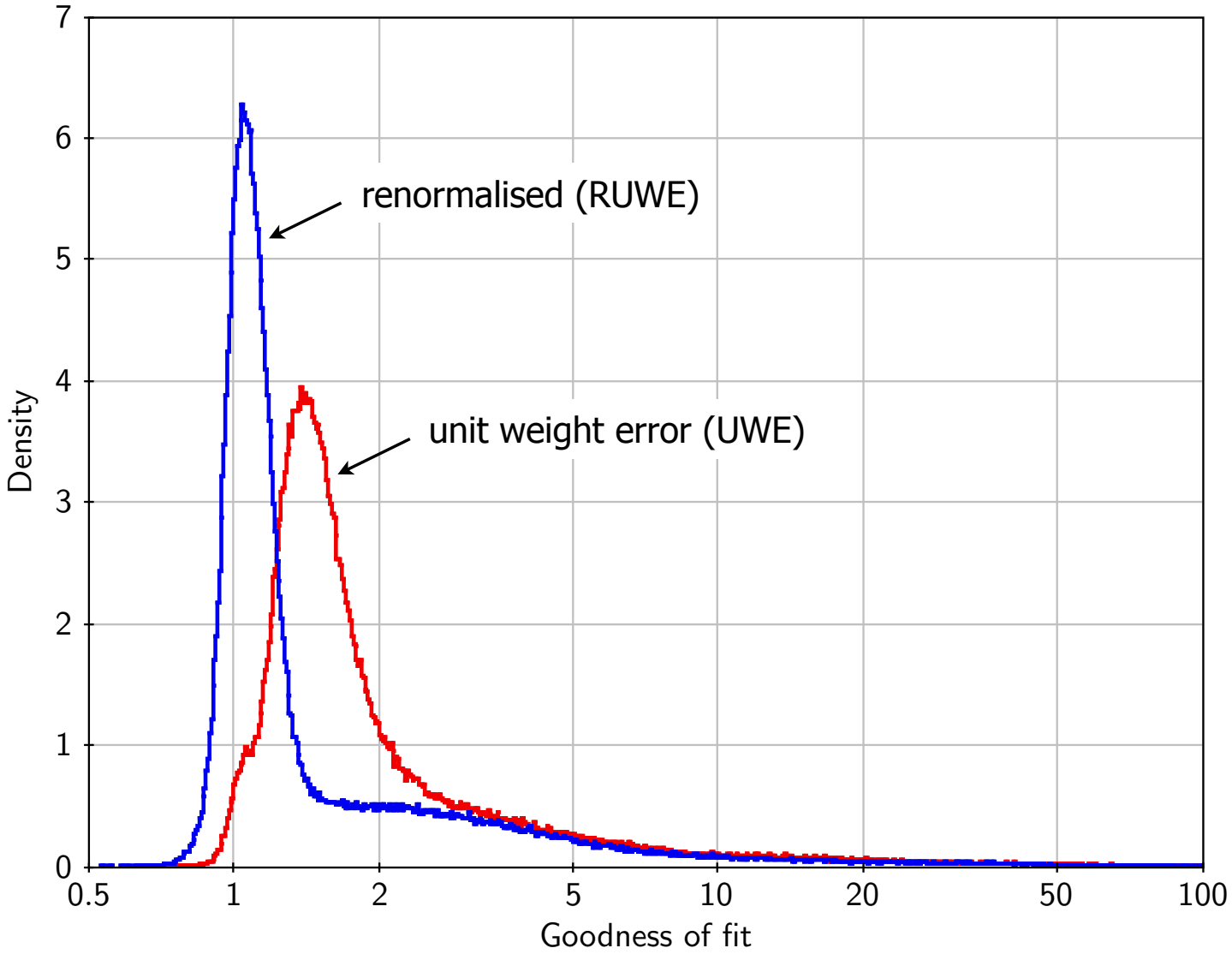

Filters for the 70% "best" sources:

UWE < 1.96

or

RUWE < 1.40

HRD filtered by UWE and RUWE

UWE < 1.96

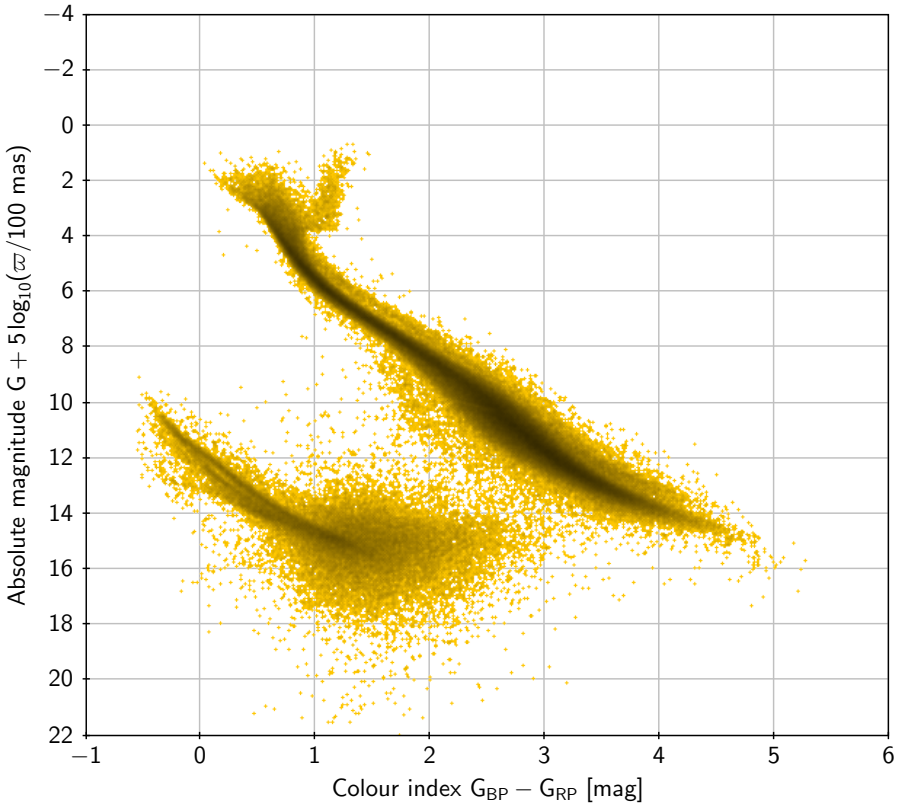

RUWE < 1.40

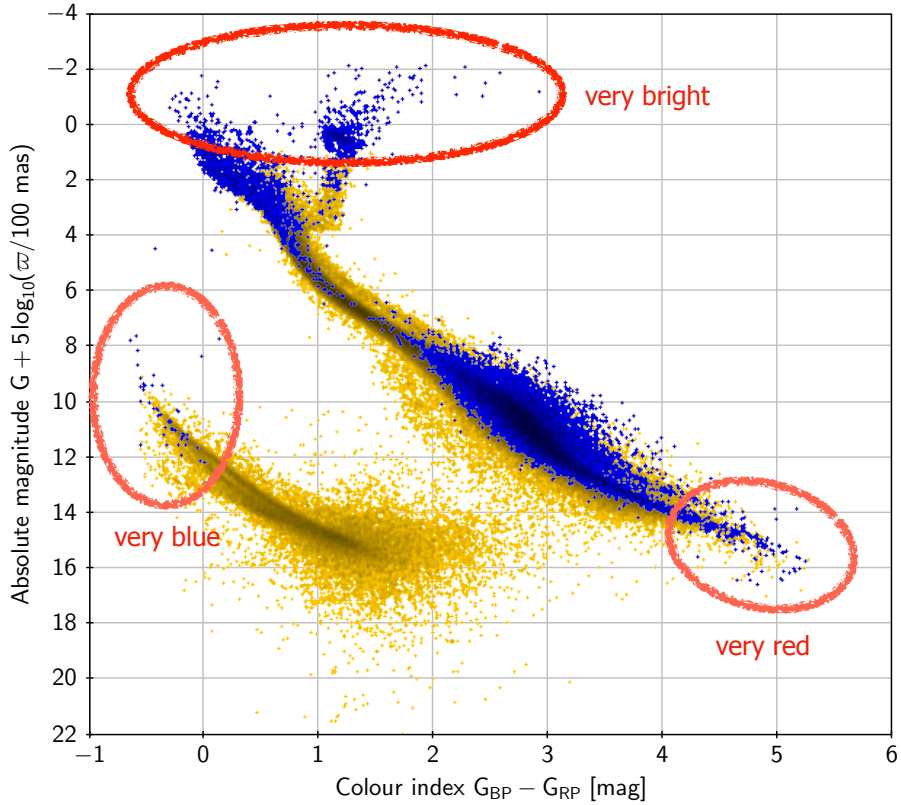

Limits chosen to retain the same number of sources

Filtering by RUWE gives a cleaner HRD

Blue dots are sources missing in the left diagram

HRD filtered by UWE

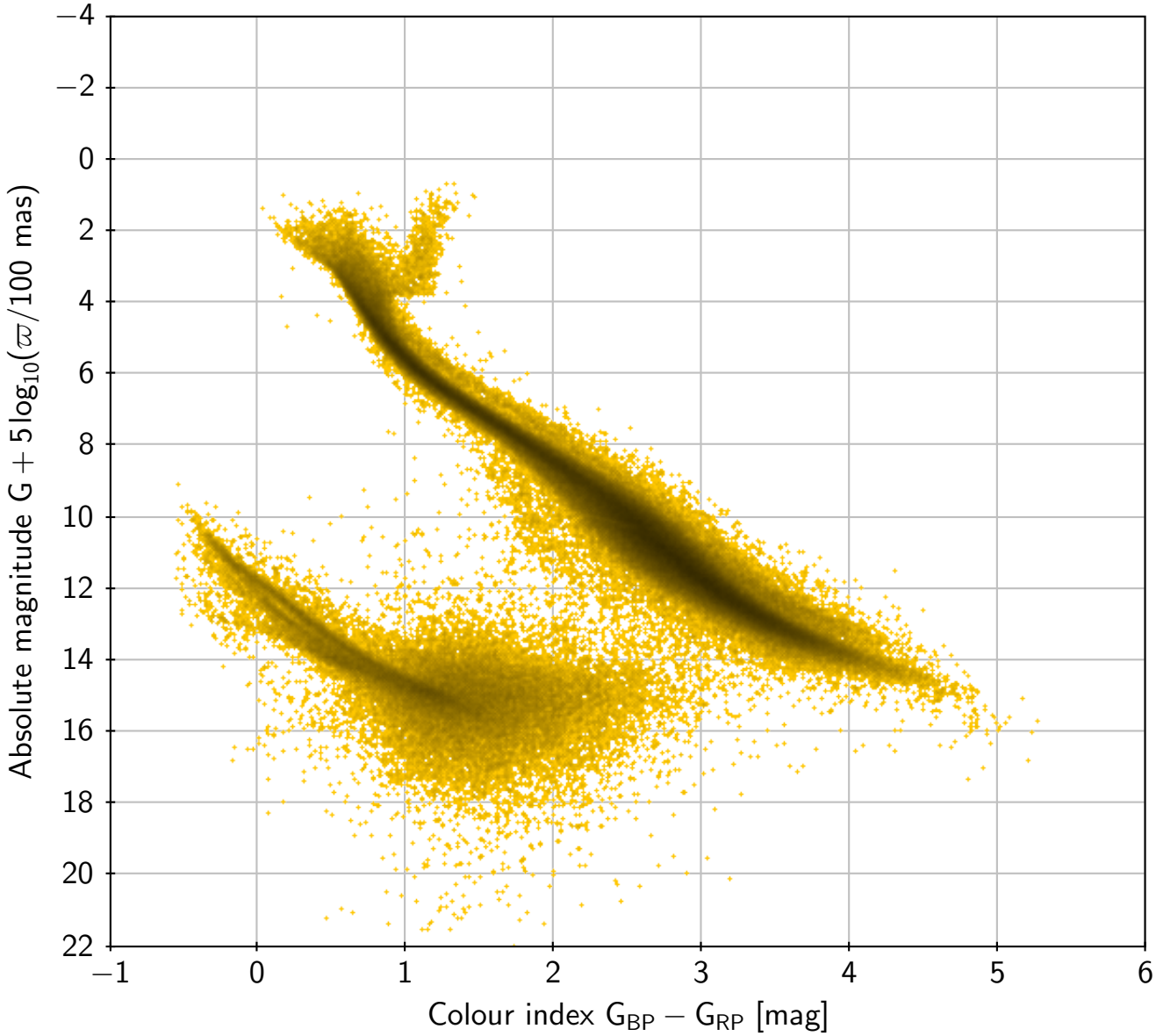

"Selection A" from L18 filtered by UWE < 1.96

(236 339 sources)

HRD filtered by RUWE

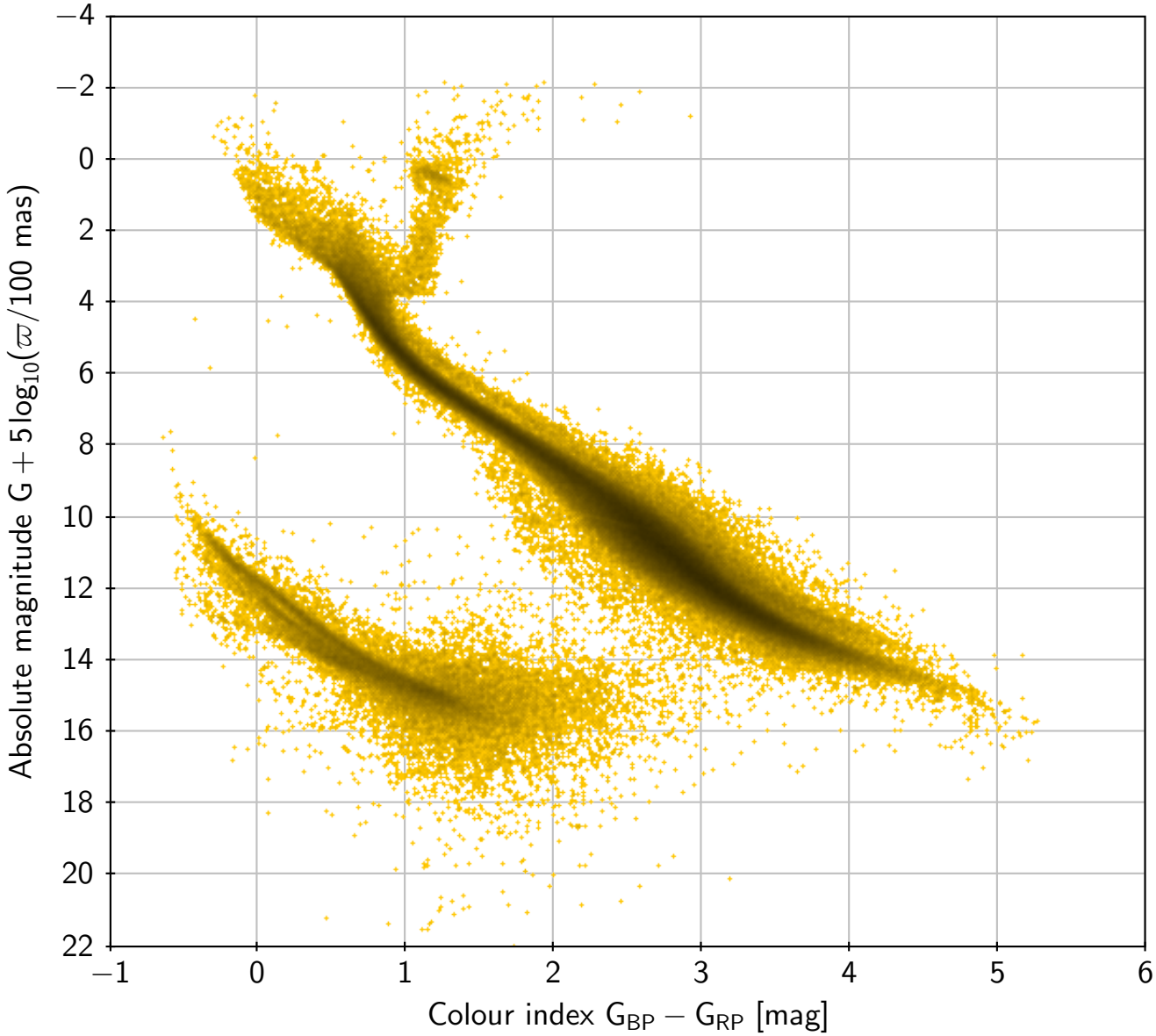

"Selection A" from L18 filtered by RUWE < 1.40

(236 684 sources)

Difference between UWE and RUWE

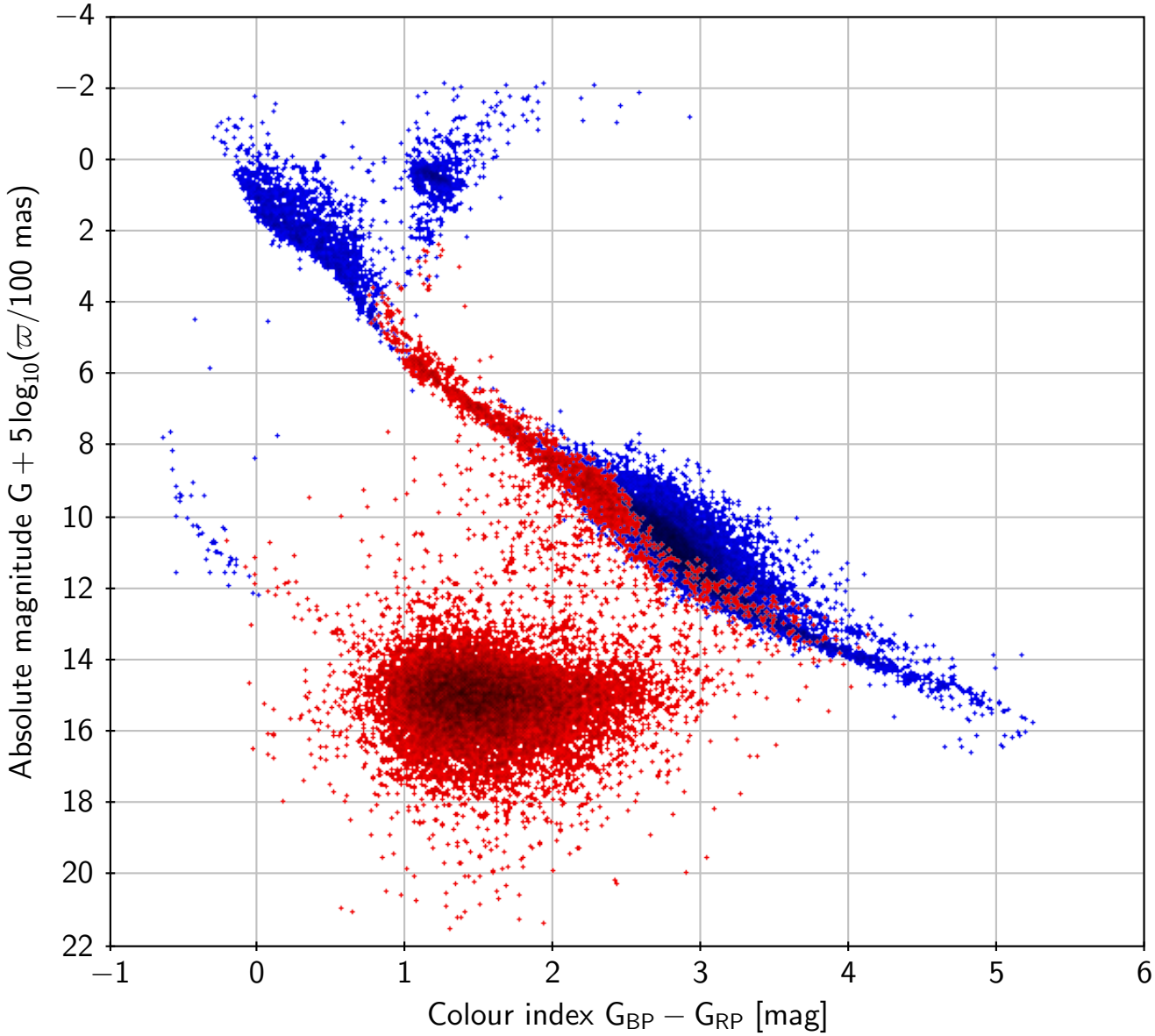

Red:
Sources removed by RUWE < 1.40 but kept with UWE < 1.96 (14 982 sources)

Blue:
Sources removed by UWE < 1.96 but kept with RUWE < 1.40 (15 327 sources)

Spurious parallaxes

Gaia DR2 contains some parallaxes that are horrendously wrong

Source ID	G	parallax	RUWE
4062964299525805952	19.63	1851.88 ± 1.29	1.44
4065202424204492928	19.88	1847.43 ± 1.87	1.01
4051942623265668864	19.35	1686.27 ± 1.47	1.63
4048978992784308992	19.78	1634.28 ± 1.97	1.50
⋮	⋮	⋮	⋮
4089303169338901632	20.35	-1621.17 ± 1.83	0.92
4059697925504813440	20.76	-1706.70 ± 1.99	1.17
4052499285375616384	20.00	-1787.00 ± 1.45	1.24
4090728411324689792	20.00	-1856.58 ± 2.72	1.72

The really big errors ($> 1''$) are probably cross-matching errors causing spurious parallax solutions – these are typically faint sources

Anomalous parallaxes

Tail of negative parallaxes

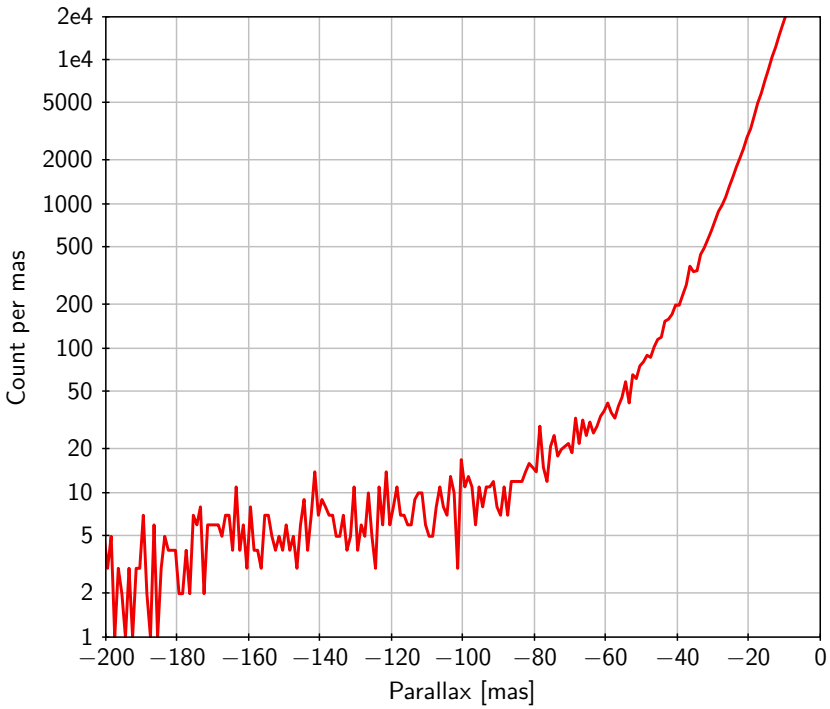

HRD for $\varpi > 10$ mas

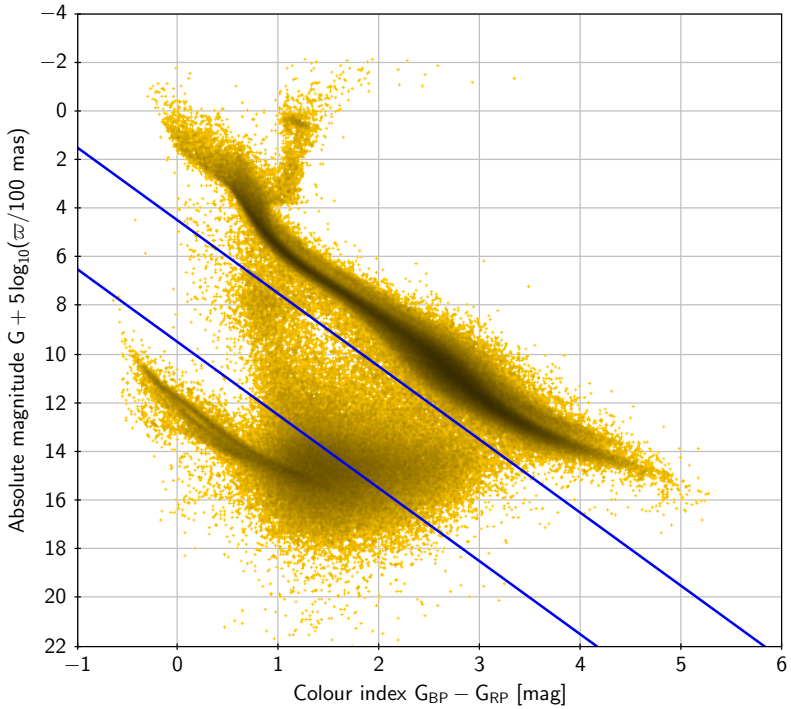

In the HRD most sources between blue lines have parallax errors >10 mas

Sources with anomalous parallaxes (wrong by ± 10 to ± 100 mas)
are usually partially resolved doubles ($\rho \simeq 0.2$–$1''$, $\Delta G < 2$ mag)
$\Rightarrow$ need dedicated processing (future releases)

Spurious parallaxes

Distribution of sources with parallax error
$|\varpi - \varpi_{\mathsf{true}}| \gtrsim 10$ mas and $G < 18.5$ mag

Negative error

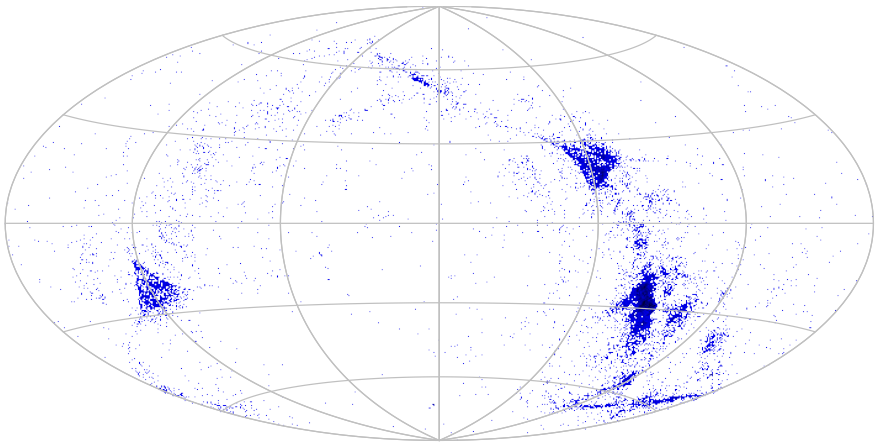

Positive error

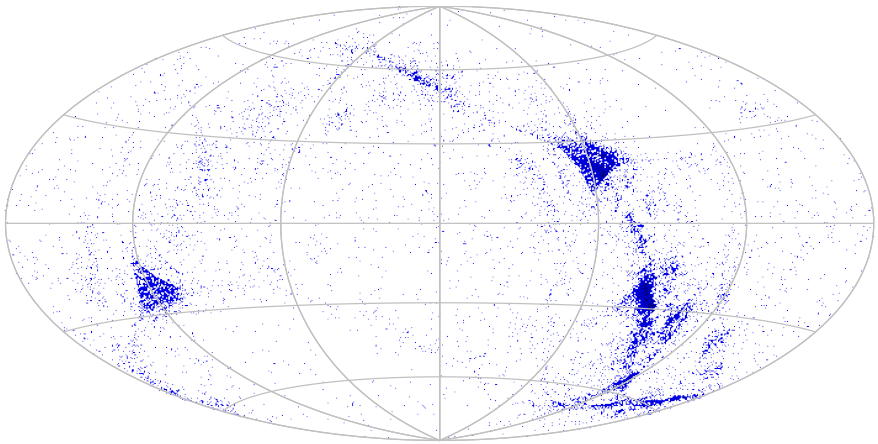

- Positive and negative errors are produced by the same mechanism
- DR2 parallax solution is more sensitive to duplicity in certain areas
- Good astrometry for these sources requires dedicated algorithms

Conclusions and outlook

- This talk focused on peculiarities and deficiencies in *Gaia* DR2
- Knowing about them will help users make optimum use of the data
- Conversely, feedback from users will help us to understand the data
- Future releases will benefit from the accumulated insight

This should not obscure the tremendous advances made:

Gaia DR2 = A giant leap for astronomy!

Formal uncertainty in parallax

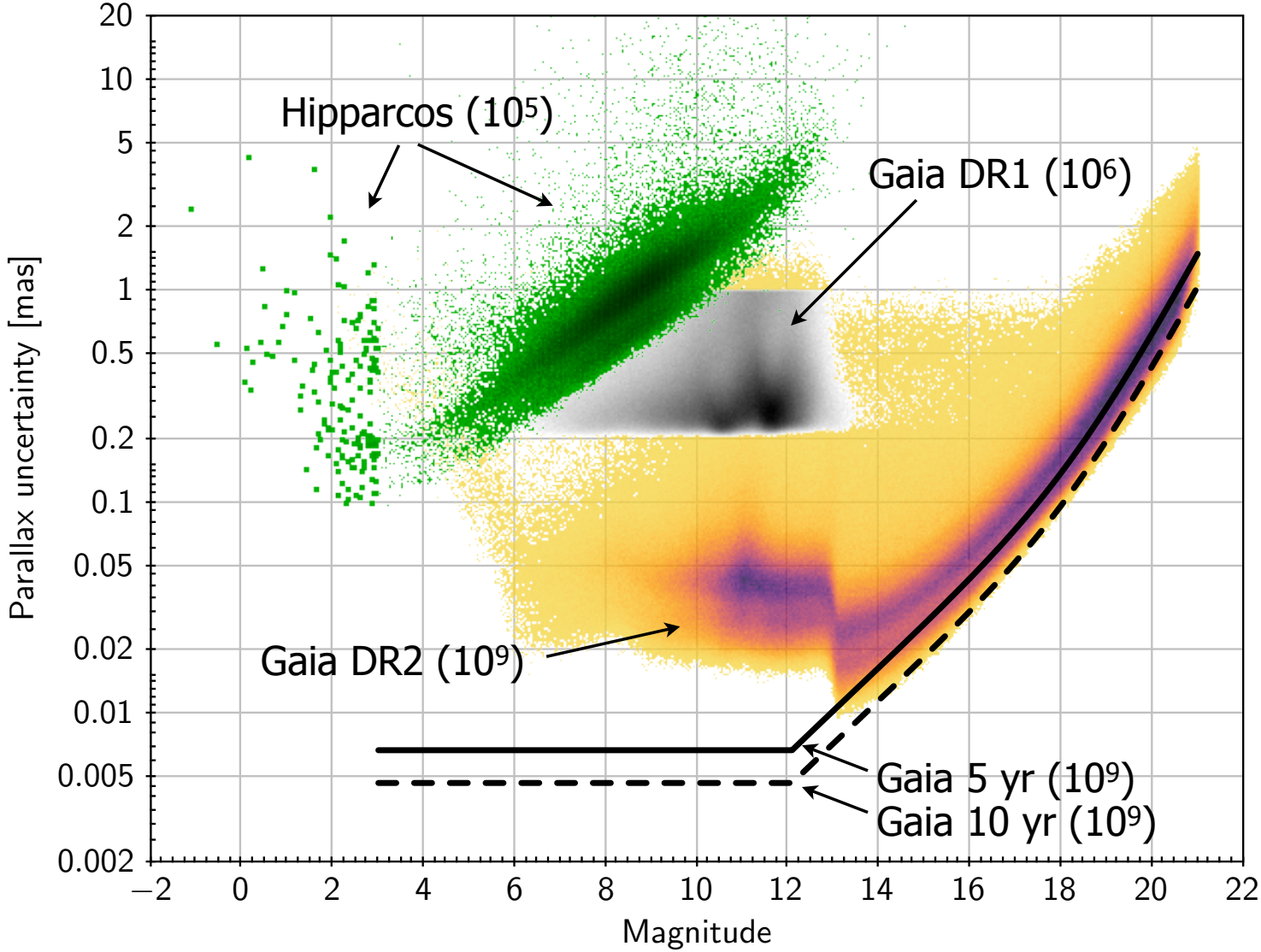

Formal uncertainty in proper motion

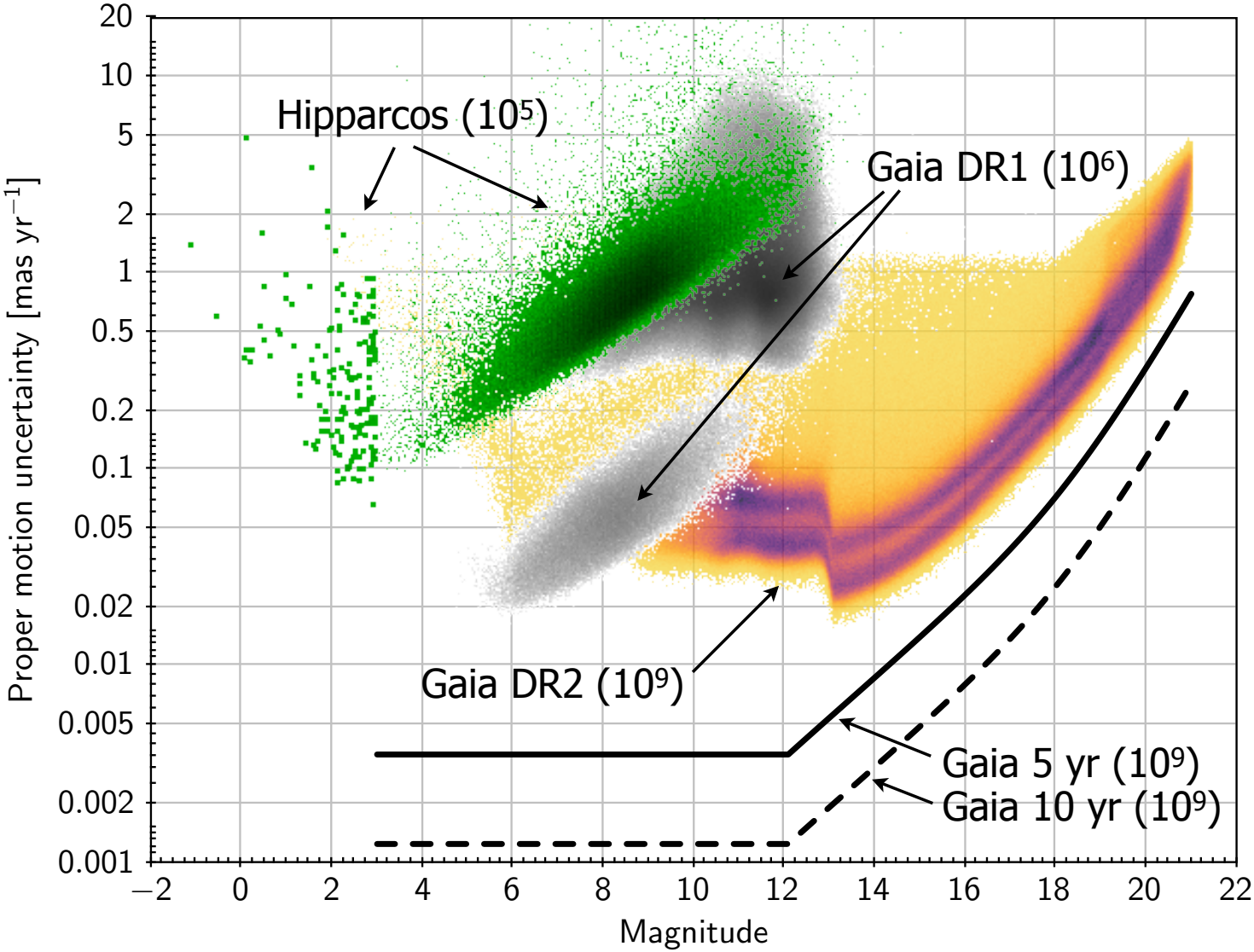

Acknowledgements

This work has made use of data from the European Space Agency (ESA) mission *Gaia* (`https://www.cosmos.esa.int/gaia`), processed by the *Gaia* Data Processing and Analysis Consortium (DPAC, `https://www.cosmos.esa.int/web/gaia/dpac/consortium`). Funding for the DPAC has been provided by national institutions, in particular the institutions participating in the *Gaia* Multilateral Agreement.

All diagrams were produced using TOPCAT (Taylor 2005).

References

References used in addition to the *Gaia* publications on slide 2:

- Riess, A.G., Casertano, S., Yuan, W., et al. (2018)
  ApJ 861, 126 (link)
- Stassun, K.G. & Torres, G. (2018)
  ApJ 862, 61 (link)
- Taylor, M.B. (2005)
  ASPC 347, 29 (link)
- Zinn, J.C., Pinsonneault, M.H., Huber, D., & Stello, D. (2018)
  arXiv e-print 1805.02650 (link)